

FINAL PUBLISHABLE REPORT

Grant Agreement number 18SIB01
 Project short name GeoMetre
 Project full title Large-scale dimensional measurements for geodesy

Project start date and duration:		June 1, 2019, 42 Months
Coordinator: Florian Pollinger, PTB		Tel: +49 531 592 5420
Project website address: www.ptb.de/empir2019/geometre		E-mail: florian.pollinger@ptb.de
Internal Funded Partners:	External Funded Partners:	Unfunded Partners:
1. PTB, Germany	9. BKG, Germany	
2. CNAM, France	10. CNRS, France	
3. GUM, Poland	11. Frankfurt UAS, Germany	
4. INRIM, Italy	12. IGN, France	
5. NLS, Finland	13. NSC-IM, Ukraine	
6. NPL, United Kingdom	14. UPV, Spain	
7. RISE, Sweden	15. WUT, Poland	
8. VTT, Finland		
Linked Third Parties: 1. OCA, France (linked to CNRS)		
RMG: -		

TABLE OF CONTENTS

1 Overview 3

2 Need 3

3 Objectives 3

4 Results 4

5 Impact 24

6 List of publications..... 25

7 Contact details 27

1 Overview

Geodetic reference frames form the backbone of all georeferencing services, providing the geospatial reference for global observations as sea level monitoring or Earth crustal movements. To strengthen the complex traceability chain, this project focussed on two issues: the creation of new long-distances references for the Earth-bound verification of space-geodetic methods like Satellite Laser Ranging (SLR) or Global Navigation Satellite Systems (GNSS) and on the measurement of the local tie vectors, the geometric connection of reference points of co-located space-geodetic telescopes. For this, the project developed specifically tailored instrumentation, like, e.g., new range meters capable to measure up to 5 km in air with sub-millimetric uncertainty, a metrologically-sound approach to GNSS-based distance measurement, or a 3D multilateration system for an outdoor working volume of 50 m which reduces the measurement uncertainty compared to state-of-the-art systems by a factor of 3. Using these systems and methods, novel reference standards like a new 5000 m reference network were established, and successful case studies for GNSS and SLR verification performed. In a unique effort, the local tie vector measurement was tackled from multiple angles at two European space-geodetic co-location sites. The novel measurement systems, but also novel measurement and analysis approaches showed their potential to push the accuracy limits further, below the targeted uncertainty limit of 1 mm and can now be applied to other respective sites.

2 Need

Monitoring changes in sea level, retreating ice sheets, and long-term tectonic motion is critical. Many Earth science measurements are referenced to the International Terrestrial Reference Frame (ITRF), the realisation of the International Terrestrial Reference System (ITRS). The ITRF is a smart combination of several services of the International Association of Geodesy (IAG), using global networks of observatories. The Global Geodetic Observing System (GGOS) of the IAG aims at aggregating all this information with other information, like gravimetric data. A network of well-instrumented sites constituting the GGOS core sites (GGOS-CS) has been set up where space-geodetic methods like Very Long Baseline Interferometry (VLBI), SLR, Doppler Orbitography and Radiopositioning Integrated by Satellites (DORIS) and GNSS receivers are co-located. In practice, The ITRF defines the scale of global geometric measurements and the long-term comparability of such data, but although the ITRS definitions use the SI, the absolute uncertainties were unknown, and the establishment of a metrological traceability chain is still a challenging task. The societal relevance of the ITRF has been demonstrated by a resolution of the UN General Assembly (GA). Many high-end applications, like sea-level or volcano stability monitoring, however, require the accuracy of the ITRF to be substantially improved in order to extract meaningful observations from global data comparisons.

Dimensional metrology was able to address two critical issues. Systematic error sources of the space geodetic methods had to be studied, understood, and compensated for to an uncertainty level of 1 mm over several kilometres. This required suitable SI-traceable references. Furthermore, the spatial correlation of the reference points of co-located geodetic instrumentation, the so-called local tie vectors, had to be determined for the joint analysis of all data. Geodetic experts had seen the need to improve the uncertainty of these complex large-scale dimensional measurements to 1 mm. This required advances in analysis, measurement strategy, and instrumentation. Novel scientific concepts and field-capable devices were necessary for SI-traceable dimensional measurements in both one and three dimensions optimised for the specific challenges that limit uncertainties previously. These measurement capabilities also improve the surveying capabilities of critical infrastructure assets.

3 Objectives

The overall objective of this project was to improve the complex traceability chain in geodetic length metrology. The specific objectives of the project were:

1. To develop and validate field-capable primary or transfer standards to disseminate the unit metre to reference baselines over distances to 5 km with the determination of the measurement uncertainty budget.
2. To develop and evaluate at least one 3D capable novel measurement device with a measurement range of 50 m for outdoor use with the determination of a targeted measurement uncertainty better than 1 μm / m.

3. To develop technologies, methods and uncertainty assessment for the Earth-bound SI-traceable verification of space-geodetic measurement technologies like GNSS or SLR over distances of at least 5 km with uncertainties of 1 mm or better and their implementation in a European reference standard.
4. To reduce uncertainty of the so-called local tie between co-located space-geodetic techniques at GGOS-CS (and all other eligible sites) by one order of magnitude to 1 mm over 200 m in real time continuous tracking. This required a coordinated effort of novel dimensional measurement systems, methodology and analysis strategies and their demonstration in pilot studies at two European GGOS-CS.
5. To facilitate the take up of the technology and measurement infrastructure developed in the project by the European geodetic measurement infrastructure by provision of European-wide access to the developed high-level references, collaboration with the established existing measurement supply chain (accredited laboratories, instrumentation manufacturers), and dissemination to standards developing organisations (ISO, IAG working groups) and end users (geodesy, surveying, high energy physics, and Earth sciences).

4 Results

Objective 1

To develop and validate field-capable primary or transfer standards to disseminate the unit metre to reference baselines over distances to 5 km with the determination of the measurement uncertainty budget.

The overall target of the GeoMetre project was a substantial improvement of the traceability chain to the SI definition of the metre of space-geodetic tools and products. As key tool, novel optical standards were developed in the project by CNAM and PTB using different technology routes that can establish reference lengths with low uncertainty in the field at the location of space-geodetic telescopes or reference baselines. They were the essential prerequisites to resolve objectives 3 and 4.

Refractive index compensation for optical distance measurements over 5 km

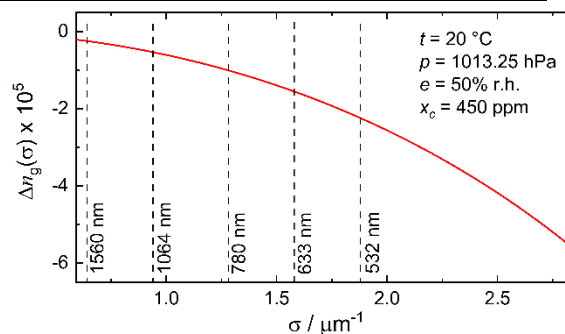


Figure 1 Difference Δn_g between the group index of refraction derived from the numerical evaluation of the determining equation from the phase index and of the prior erroneous solution¹.

One major challenge for the optical distance metres when used for the surveying of long distances lies in the determination of the air refractive index n . Usually, it is calculated using the semi-empirical Edlén's equation that depend on the vacuum optical wavelength, but also on the air temperature T , the pressure p , the partial pressure of water p_w , and the CO_2 content x . For most geodetic instrumentation, the group index of refraction $n_g = n + \sigma \frac{dn}{d\sigma}$ is the relevant quantity. Since 1999, the International Association of Geodesy (IAG) officially recommends the algorithm published by Ciddor and Hill² in 1999 for use in geodetic measurements. During the project, working on the two-colour framework discussed below, PTB discovered a subtle, but highly unfavourable sign error in their published algorithm which impacts the group index of refraction by several parts-per-million (ppm), depending on the carrier wavelength (Figure 1).

In general, an accuracy of 1 mm over 5 km would require a knowledge of the temperature at 0.2°C , which is nearly impossible to achieve in practice using classical sensors. To overcome this limitation, the so-called two-

¹ Reprinted from Pollinger, F. (2020) Appl. Opt. 59, pp. 9771-9772

² Ciddor, P. E., and Hill, R. J. (1999) Appl. Opt. 38, pp. 1663-1667

colour method first described by Earnshaw and Owens³ can be used. This consists in measuring two optical distances simultaneously at two different wavelengths. Thus, the distance l measured by a two-colour instrument, i.e. the length of the wave paths also called air index compensated distance (first velocity correction), is calculated as follows:

$$l = d_{\lambda_1, n=1} - \frac{n(\lambda_1, T, p, x, p_w) - 1}{n(\lambda_2, \dots) - n(\lambda_1, \dots)} (d_{\lambda_2, n=1} - d_{\lambda_1, n=1}) \quad (1)$$

with $d_{\lambda_1, n=1}$ and $d_{\lambda_2, n=1}$ the two optical distances measured at the wavelengths λ_1 and λ_2 . In dry air, the fraction term in Eq. (1), the so-called A -factor, loses its dependence on the environmental parameters and depends only on the optical vacuum wavelengths. Thus, an auxiliary measurement of the environmental parameters by sensors, prone to grow in uncertainty with the length of the measurement, is in principle not necessary anymore, only an accurate knowledge of the optical path lengths and the vacuum wavelengths of the optical beams. This approach can be extended to humid air if the water vapor can be independently determined with a moderate requirement on the associated uncertainty (for a group index-based distance measurement, the water vapour pressure p_w needs to be known with an accuracy of 200 Pa, or 7.5% relative humidity at 20°C). The disadvantage of the method, however, is the fact that all uncertainties of the optical path measurement are scaled by the A factor, i.e., depending on the wavelengths used and the method, a factor of 20 up to 150, when applying Eq. (1.1).

The project targeted measurement systems for distances over 5 km which were flexible in use. The need to maintain sensor networks over 5 km would severely limit their applicability. Therefore, both systems described in the following pursue the implementation of the two-colour compensation scheme. To soften the impact of the associated unfavourable uncertainty scaling, a highly accurate measurement of the optical path distance is required. The project pursued two different technology routes to overcome this challenge.

The Arpent system

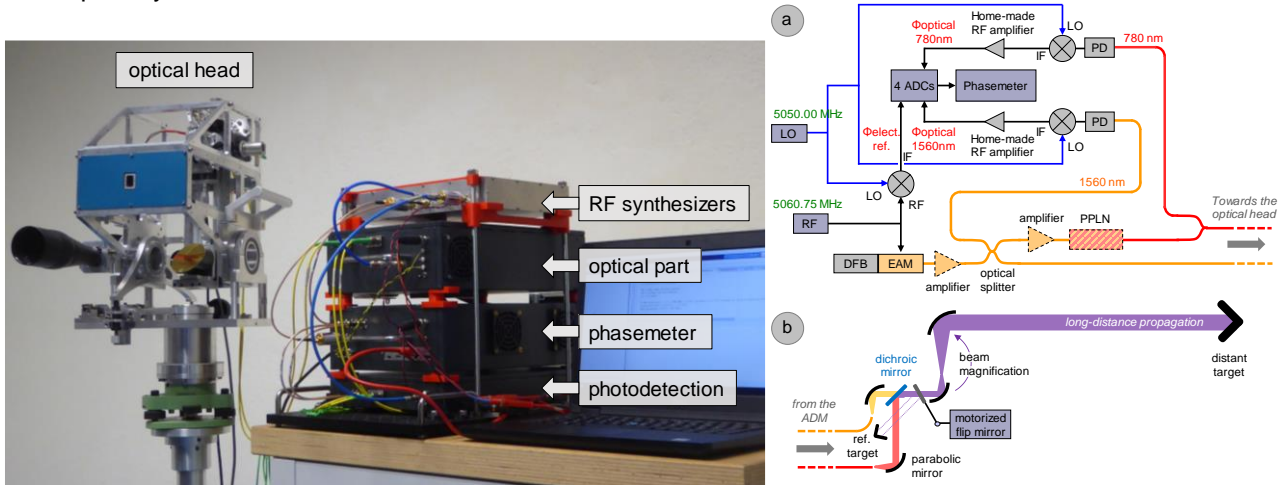


Figure 2 Left: photograph of the two-colour absolute distance meter Arpent, the main functional units labelled. Right: schematic design of the Arpent optical system: a) optical source and phase meter, b) measurement head.⁴

The Absolute Distance Meter (ADM) Arpent developed by CNAM is based on a well-known technique: a light beam is intensity modulated by a RF carrier, propagated in air up to a distant target, retroreflected, and finally detected by a photodetector. The distance to be measured is thus proportional to the phase delay ϕ measured between the RF carrier detected after propagation in air and the emitted one.

$$D = \frac{1}{2} \left(\frac{\phi}{2\pi} + k \right) \times \frac{c}{n \times f_{RF}} \quad (2)$$

with c the speed of light in vacuum, n the group refractive index of air, f_{RF} the frequency modulation of the light, and k an integer number corresponding to the number of times that the phase has rotated by 2π during its propagation. At the beginning of the project, a first laboratory version working with a single wavelength was available. The concept has then been developed towards a two-colour system, working at 779.8 nm and 1559.6 nm, which implies a rather large A -factor and thus, unfavourable uncertainty scaling for the measurement. Nevertheless, the wavelengths of the prototype are interesting due to the wide availability of

³ Earnshaw, K. B., and Owens, J. C. (1967) Journal of Quantum Electronics 3, pp. 544–550.

⁴ Reprinted from Guillory et al. (2022), Proc. JISDM 2022, <http://doi.org/10.4995/JISDM2022.2022.13786>

affordable fiber-optic components in this range, especially at 1560 nm, which is used in the telecommunication industry. The developed prototype is presented in Figure 2. It is compact, easily transportable, and thus ready for measurements in the field.

Table 1 Uncertainty budget for distance measurements with the Arpent distance meter (single colour measurement).

uncertainty component	source of uncertainty	value	contribution
$u_{f_{RF}}$	values of the RF carriers	5060.75 MHz	$4.8 \times 10^{-10} L$ (μm)
$u_{crosstalk}$	presence of crosstalk	SCR > 60 dB	< 3.3 μm
$u_{AM/PM}$	variations of the signal amplitude	amplitude variations < 15 dB	0.6 μm
u_{random}	random noise on the phase measurement	~0.4 mrad	2.0 μm at 780 nm and 1.8 μm at 1560 nm

Table 2 Summary of the uncertainty contributions due to the mechanics to the Arpent system.

uncertainty component	source of uncertainty	uncertainty contribution	
		optical head	target
$u_{\text{Tribrach, positioning}}$	position reproducibility of the instruments on the Tribrach	5 μm	5 μm
$u_{\text{Tribrach, centering}}$	difference between the vertical axis of the instruments and the reference mark	9 μm	15 μm
$u_{\text{levelling}}$	reproducibility of the vertical axis of the instruments	31 μm	26 μm
u_{offset}	Instrument offsets of -132.3221 mm (λ_1) and -132.3264 mm (λ_2)	24 μm	
u_{gimbal}	errors in the gimbal mechanisms (transit offset, beam offset, ...)	2 μm	5 μm
$u_{\text{long-term drift}}$	long-term effects (drifts due, for example, to thermal expansion)	~20 μm for a single wavelength and 3.7 μm for the distance difference	

During the project, CNAM developed a sophisticated uncertainty model for the Arpent system. First, the uncertainty components of the ADM for each wavelength are first considered separately. Four sources of error have been identified: the modulation frequency ($u_{f_{RF}}$), the crosstalk effect ($u_{crosstalk}$), amplitude-to-phase coupling $u_{AM/PM}$ and random noise u_{random} . CNAM studied their influence carefully during the project, the results being summarized in Table 1. The global uncertainty of the ADM, taking into account these different sources of uncertainty, can be calculated for a signal-to-crosstalk ratio (SCR) higher than 60 dB to a measurement uncertainty of 4.5 μm ($k=1$) over 5 km. Over short distances, the uncertainty is even lower since the received RF signals is higher after propagation in the air and the SCR is so also higher.

In case of an absolute measurement, additional uncertainty sources must be taken into account, such as those depending on the mechanical parts, or the on the target. CNAM investigated both contributions with great care as well. The results for the mechanical contributions are summarized in Table 2. Adding all mechanical contributions to the uncertainty of the single distance measurement, CNAM obtains an uncertainty for the measurement at a single wavelength, $d_{\lambda 1, n=1}$, of 55 μm . This number, however, is only valid for an assumed perfect refractivity compensation, or a measurement in vacuum. If the two-colour method is used for the compensation of the index of refraction, the uncertainty of the refractivity-compensated distance meter is better than 0,65 mm at $k=1$ for a short range such as 1 km where the SCR is better than 60 dB. More generally, the uncertainty is better than 0.95 mm up to 5 km.

During the project, there have been multiple experiments to investigate and validate the Arpent system, including, inter alia, indoor comparisons on a 50 m interference comparator, measurements at the geodetic co-location sites of Wettzell, Germany, and Metsähovi, Finland together with BKG and NLS (see objective 3), measurements at the EURO5000 baseline and at the CERN reference monitoring field together with IGN, UPV, WUT, GUM, and CERN (see Objective 3). Here, we want to report the results of the measurement campaign at the the world-wide unique Nummela Standard Baseline as benchmark baseline run by NLS. The

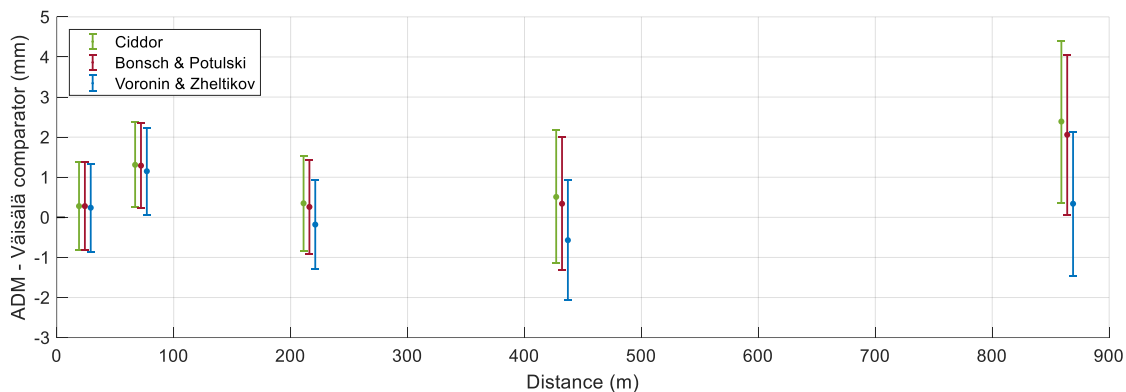


Figure 3 Comparison of the CNAM absolute distance metre with the Väisälä comparator values provided by NLS. The results, obtained for a received RF power higher than -15 dBm, correspond to the average value of raw data with confidence intervals of $\pm 2\sigma$ ($k=2$).

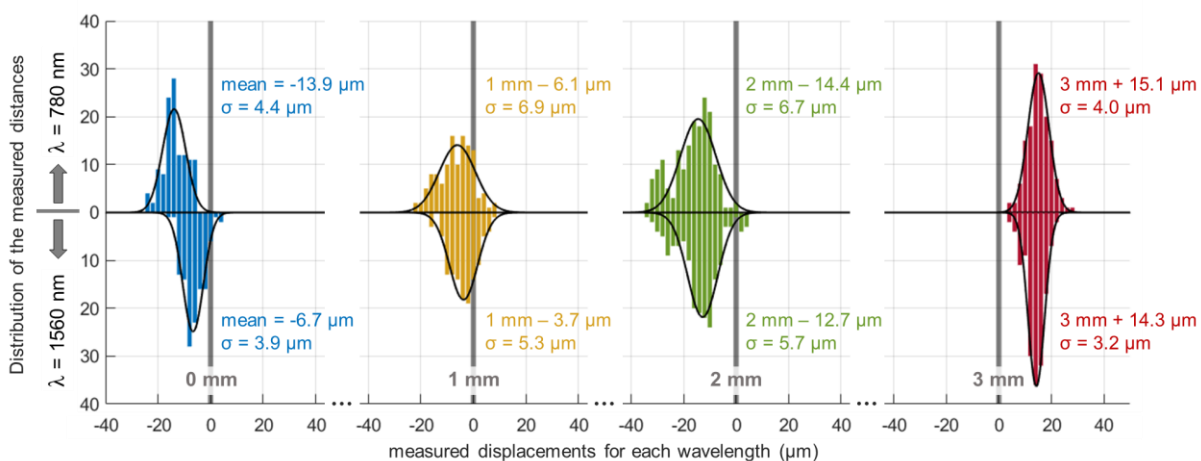


Figure 4 Distribution of recorded distances when a distant corner cube is moved by step of 1 mm, 5.4 km away from Arpent. This demonstrates a resolution around $5 \mu\text{m}$.⁵

baseline has been in operation since over 100 years, and been monitored by white-light interferometry, the so-called 'Väisälä interferometer' since then. NLS provides reference values of distances between all pillars with an uncertainty of $310 \mu\text{m}$ ($k=2$). This baseline is hence traceable to the SI unit meter with a proven very low uncertainty and serves as a global gold standard for long-distance measurement verification. Using the formula by Voronin and Zheltikov⁶, the observed deviations of the Arpent measurements are well within the measurement uncertainty of the reference values (see Figure 3). The convincing performance of the optical system is also demonstrated in Figure 4. A corner cube in 5.4 km was moved by a translation stage with steps of 1 mm per minute in urban environment in cloudy weather without sunlight. Measurement results demonstrate a resolution around $5 \mu\text{m}$.

⁵ Reprinted from Pollinger F. et al. (2023) Appl. Geomatics, <https://doi.org/10.1007/s12518-022-00487-3>

⁶ Voronin, A. A., and Zheltikov A. M. (2017) Scientific Reports 7, 46111.

The TeleYAG-II interferometer as alternative approach

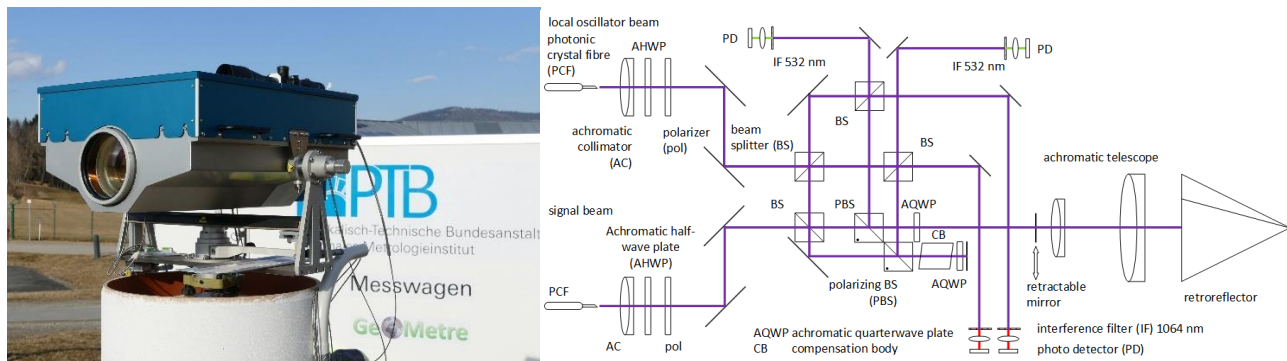


Figure 5 Left: Interferometer head of the TeleYAG-II measurement system mounted on a geodetic pillar at the geodetic co-location site at Wettzell, Germany. The laboratory trailer can be seen in the background. Right: functional scheme of the heterodyne two-colour absolute distance interferometer.

The availability of a standard that was able to measure over longer distances up to 5 km with low uncertainty and well understood traceability to the SI-definition of the meter was essential for the completion of the Objectives 3 and 4 of the GeoMetre project. Therefore, Objective 1 was also tackled by PTB following an alternative technology path. Based on their experience with heterodyne absolute interferometers, they pursued multi-wavelength interferometry as fundamental measurement principle of their so-called 'TeleYAG-II' system. As optical sources, PTB worked with frequency-doubled Nd:YAG lasers whose frequency difference is stabilized by an optical-phase locked loop based on a by a field-programmable gate array (FPGA). This powerful scheme allows a flexible choice of synthetic wavelengths. The range of non-ambiguity can be tuned by combining measurements from several metres down to 7.5 mm. The beam modulation for the heterodyne detection scheme was realized by an all-fibered setup. PTB also developed a fibre-moderated scheme to superimpose their two optical carrier wavelengths of 532 and 1064 nm, using photonic crystal fibres (PCF). These measures provide improved stability and control of the optical source compared to previous free-space versions. The FPGA-based phase meter was demonstrated to achieve single-digit picometer resolution for 40 kHz bandwidth averaging of synthetic signals. The optics and mechanical mount of the measurement head (see Figure 5) were very carefully designed as well. All optical components (see Figure 5) were carefully selected for achromatism with respect to the 532/1064 nm colour combination and achromatism. The achromatic lens system was custom designed for the targeted range of up to 5 km with an exit aperture larger than 120 mm. The mechanical frame and all opto-mechanic components were designed for thermal robustness and manufactured and assembled in part under surveillance by coordinate-measurement-machines (CMM) to reduce constructional sources of uncertainty.

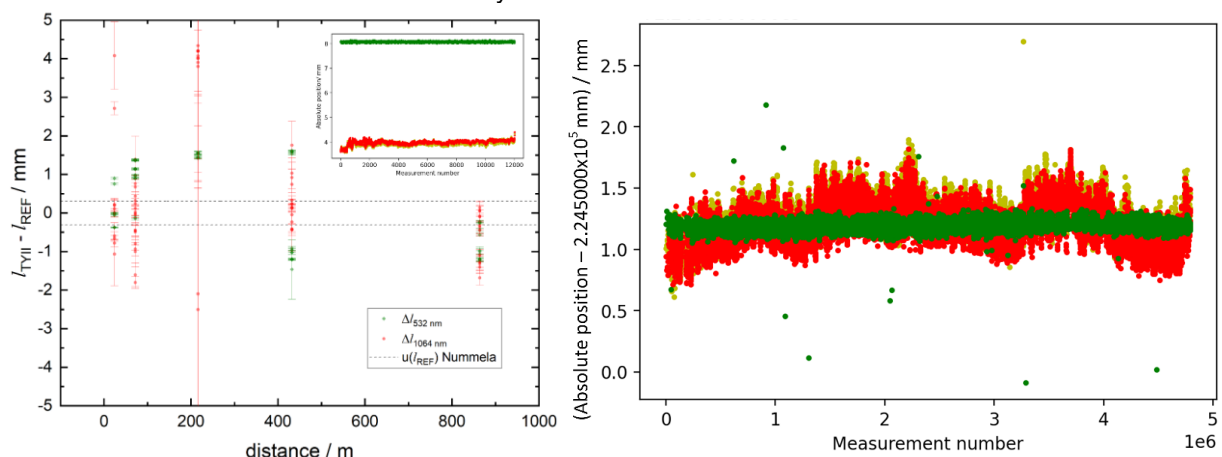


Figure 6 Left: Preliminary results from the measurement campaign at Nummela Standard Baseline. The circles represent the median positions derived for the 1064 and the 532 nm measurement, plotted as deviations from the Väisälä reference values. The error bars indicate the standard deviations for 1 ms averaging. The inset depicts an exemplary fine measurement result at 432 m at 532 nm (green) and 1064 nm (red, gold) uncorrected for the imbalanced glass path and for the interferometer dead path. Right: agreement of absolute positions signals at the WUT200 campaign after inclusion of the glass compensation body to the reference path. 532-nm data is depicted in green, 1064-nm data in red and gold

Similar as the Arpent system, the TeleYAG-II system was carefully studied and validated at several locations together with several partners during the GeoMetre project as well, promoting constant improvement of the system: at Metsähovi and Nummela with support by NLS, at Wettzell supported by BKG, and at the new 250 m reference baseline WUT200 in Warsaw in a joint measurement campaign with WUT, GUM, INRIM, and VTT. The preliminary results of the Nummela data depicted in Figure 6 shows on one hand a good performance of the system, but also imply remnant problems. The inset, e.g., shows a constant offset in the order of 4.1 mm between infrared and visible measurement results. The subsequent inclusion of a glass compensation body into the reference path (CB in Figure 5) led to a better balance of the glass paths in the interferometer. Data taken a year later at the WUT200 baseline depicted in Figure 6 demonstrate the better coincidence of 532 and 1064 nm data. Due to in part COVID 19 pandemic-related delays, the TeleYAG-II prototype system was completed only about 15 months before the end of the GeoMetre project. Not surprisingly, it required a lot of optimization work. In a steep learning curve, PTB learned to operate and optimized their system during the various measurement campaigns in the project. Thus, unlike the Arpent system, the measurement uncertainty of the TeleYAG-II system was not fully characterized during the project. But the work will be continued at PTB.

Summary

Objective 1 was highly challenging, and the Consortium ran into multiple scientific and physical problems. Both Arpent and TeleYAG-II are scientifically fascinating instruments and still pose a number of scientific challenges. The efficient characterization and validation of both systems was only possible due to the good collaboration of multiple partners in the project, which also provided access to characterization at world-leading facilities like the Nummela standard baseline maintained by FGI or the EURO5000 and WUT200 baselines developed in this project by WUT and GUM. The Arpent system has successfully demonstrated a high-accuracy measurement over 5 km and a full measurement uncertainty budget could be provided. The Objective to develop and validate field-capable primary or transfer standards to disseminate the unit metre to reference baselines over distances to 5 km with the determination of the measurement uncertainty budget could hence be achieved. Both systems successfully served their purpose for the completion of the subsequent objectives.

Objective 2

To develop and evaluate at least 1 3D capable novel measurement device with a measurement range of 50 m for outdoor use with the determination of a targeted measurement uncertainty better than 1 $\mu\text{m}/\text{m}$.

Space-geodetic observations like Satellite-Laser-Ranging (SLR) or Very Long Baseline Interferometry are made by large telescopes. To transform their observations from their internal frame of reference to a global one, their internal reference points must be determined in the external frame. This corresponds to a challenging (very) large volume 3D measurement problem outdoors, given the targeted overall uncertainty of these reference points by less than 1 mm in 3D. Novel instrumentation optimized for this problem would significantly simplify this task. The Consortium therefore worked on two 3D capable high-accuracy multilateration systems, as well as on novel auxiliary instrumentation to reduce the environment-induced measurement uncertainty for these measurements.

The DistriMetre system

The DistriMetre system is a multilateration system that was originally developed for large volume applications indoors in the frame of the EMPIR 17IND03 LaVA project. During this project, it was developed further towards outdoor capability, characterized in uncertainty, and deployed outdoors for the determination of the reference point of a radio antenna. The basis of the DistriMetre system is an ADM working at 1550 nm. It uses a robust ranging technique based on optical signal modulated with radio frequency (RF). The signal modulation scheme is identical to the one used for the Arpent system and is discussed in more detail in Objective 1. This optical telemetric source provides four fibre output ports, which feed four compact optical heads. These heads consist of a gimbal mechanism enabling beam rotation in any direction around an invariant point in space. For a multilateration measurement, these heads probe the same target. For common visibility, i.e. secure reflection of the emitted beam back from the target, either a rotatable open retroreflector or a $n=2$ glass sphere can be used. The system is depicted in Figure 7.

CNAM very thoroughly investigated the 3D measurement uncertainty of system. For this, they studied the uncertainty of the telemetric system, the index of refraction, the geometric errors due to the mechanical configuration of the measurement heads and the influence of the multilateration analysis and configuration. The uncertainty contributions to the telemetric unit are similar to the uncertainty of the distance measurement of the Arpent system (see Table 1). The telemetric unit of the DistriMetre system relies on classic refractivity

compensation. This requires reasonably stable measurement conditions (e.g. cloudy sky), and a performant grid of environmental sensors. For the uncertainty target of $1 \mu\text{m} / \text{m}$, the temperature needs to be known significantly better than 1 K. This is a challenge outdoors, but for reasonably stable measurement conditions, like cloudy sky or night-time, this can be achieved using well distributed environmental sensors. Furthermore, as any manufactured mechanical part, the gimbal systems and the whole mechanical setup is not perfect. CNAM identified four major sources influencing the 3D measurement of the system, characterized them and derived conclusions on their impact for the overall measurement uncertainty. They are summarized in Table 3. If properly corrected, the contribution of the geometric errors can be contained to $9 \mu\text{m}$.



Figure 7 The multilateration system DistriMetre consists of four measurement heads and rotatable corner cubes or glass spheres as targets⁷. The right picture shows a measurement head mounted outdoors on a roof for the determination of a radio antenna reference point.

Table 3 Summary of uncertainty contributions to the DistriMetre 3D measurement due to mechanical influences.

Source	Description	Error induced on the difference
Misalignment of the gimbal mechanism of the measurement head	Beam offset and beam tilt	$< 250 \text{ nm}$
	Transit offset of the head	$< 2 \mu\text{m}$ after correction
Misalignment of the gimbal mechanism to the target	Target offset	$< 9 \mu\text{m}$
	Transit offset of the target	$< 2 \mu\text{m}$ after correction
Difference between the measured and the mechanical distance	Distance offset (no impact on multilateration)	can be corrected
Limited Resolution of the pointing system	Pointing error	Negligible for the DistriMetre system

For the 3D measurement, the positions of targets and measurement heads in 3D space must be determined from the observed single distance measurements. This procedure can be solved using a self-calibrating multilateration algorithm. The propagation of the input uncertainties through this algorithm is non-trivial. The achievable uncertainty also strongly depends on the measurement configuration. CNAM derived analytical uncertainty treatment and compared it to an uncertainty assessment based on Monte-Carlo simulations and experimentally obtained standard deviations. For macroscopic measurement volumes, exemplary uncertainties between 10 and $22 \mu\text{m}$ were demonstrated.

⁷ Reprinted from Guillory et al. (2022) Metrology 2, pp. 241 - 262

Absolute3D measurement system

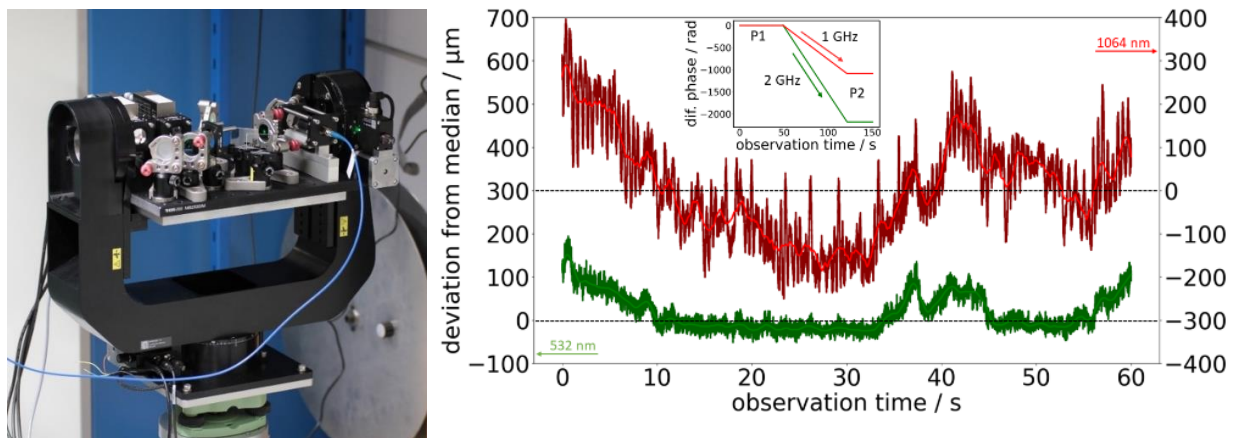


Figure 8 Left: Setup of one Absolute3D sensor head. b) Typical distance measurement data with the Absolute3D system over 26 m indoors. The data shows the deviation from the median value for the position data obtained from the synthetic wavelengths at 532 nm and 1064 nm. The lines indicate a moving average over 1 s⁸.

Gradients of the air refractive index imply an uncertainty of the scale. As discussed before, the two-colour method discussed before can be an approach to overcome this problem. Therefore, PTB explored the possibilities of two-colour 3D measurement system based on multi-wavelength interferometry, the so-called Absolute3D system. A clean separation of each phase signal is needed for a multi-wavelength measurement, which brings a considerable effort in the signal evaluation. In case of the TeleYAG-II system, PTB used a complex heterodyne interferometer setup for this, implying a huge effort on the optical side. This approach is not easily scalable and thus not the best option for a multi-lab setup which requires at least four measurement heads. PTB investigated a sinusoidal modulation technique as an alternative electronic modulation scheme which enables a much more compact measurement head. A simple Michelson setup is sufficient for the optical implementation of the interferometer. As can be seen in Figure 8, PTB mounted this compact measurement head on a commercial gimbal system for their laboratory prototype of a 3D-capable measurement system. The complex modulation and demodulation scheme was developed and characterized during the project, and PTB performed verification measurements in their 50 m indoor laboratory. The exemplary data shown Figure 8 for a distance of 26 m shows for both signals at 532 and 1064 nm a clearly correlated common behaviour due to the environmental influences. In future work, PTB will work on the further reduction of nonlinearity effects which currently deteriorate the quality of the two-colour compensated signal.

Acoustic thermometry

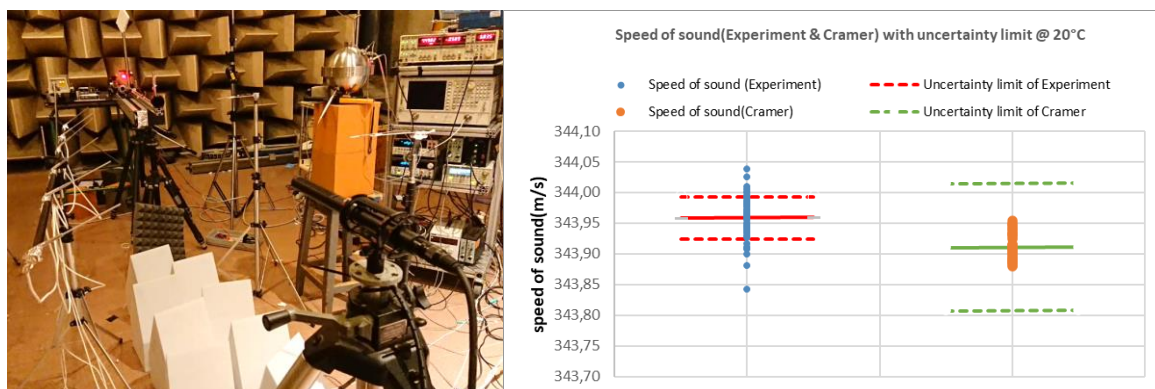


Figure 9 Left: Experimental set-up for the measurement of the speed of sound. At the background/left the carriage carrying the loudspeaker is visible, at the foreground on the right the microphone on the tripod, at the left the array of resistance thermometers, and top right the experiment with the spherical resonator. On the floor foam absorbers for reducing acoustic reflections. Right: Results of a set of measurements of the speed of sound u carried out at the anechoic chamber at INRIM for an air temperature of 20 °C.

⁸ Reprinted from Sauthoff et al. (2023) Proc. JISDM 2023, <http://doi.org/10.4995/JISDM2022.2022.13635>

Beyond the two-colour method alternative approaches to more effective refractive index compensation pursue concepts to measure the effective temperature along the beam itself using some air property, which has a known dependence on temperature. A promising approach is the exploitation of the strong air temperature influence onto the speed of sound u . The advantage of the method is given by the fact that with a single measurement it is possible to measure the average temperature along the same optical path involved in the optical measurement. INRIM has developed two acoustic thermometers based on different principles for different distance ranges. The first is based on the emission of a continuous acoustic wave received by a microphone and by measuring the phase delay between the source and the receiver depending on the speed of sound u . The second is based on the emission of a short sound burst and the measurement of the time delay between the source and the receiver again depending on u . The continuous wave method has higher resolution but is limited to medium distances or to quiet environments such as closed industrial buildings, while the pulsed method is suitable for long distances. The two thermometers have been built and tested in relevant environments. In particular, the long-distance thermometer has been compared with temperature measurements performed with complementary methods such as oxygen spectroscopy by VTT and a distributed array of thermometers. The realization of an acoustic thermometer based on a continuous wave proved capable of measuring the temperature of air with an uncertainty less than 0.1 °C up to distances of 60 m in a quiet environment, while the acoustic temperature measurement based on acoustic pulses demonstrated an air temperature measurement with an uncertainty less than 0.2 °C up to distances of 200 m in an open environment.

A complementary activity carried out by INRIM is the accurate determination of the speed of sound. Indeed, the known formulas (Cramer and Zuckerwar) that correlates the speed of sound with temperature (and vice versa), are known with an uncertainty not less than 300 ppm, whereas the uncertainty needed to reach an uncertainty level of 0.1 °C goal corresponds to an uncertainty of less than 170 ppm. An experimental set up was dedicated to the determination of the speed of sound with an uncertainty of 100 ppm in a relevant temperature interval. The experiment consists in measuring the delay phase of a continuous wave device while the distance between the source and the receiver is moved under the control of an interferometer. This allows to measure the acoustic wavelength with a high accuracy. At the same time the temperature of air is measured with several calibrated thermometers along the path. A second device, based on a spherical acoustic resonator, already used to measure the Boltzmann constant, measures the speed of sound in the same environment. The comparison between the experiments allowed to assess the speed of sound in a certain interval of temperature with the required uncertainty. For the relevant environmental conditions in the range of 10 to 30 °C, the relative uncertainty of the respective Cramer and Zuckerwar expressions was lowered to 100 ppm, allowing to measure the temperature of air through the speed of sound with an uncertainty of 0.06 °C.

Spectroscopic thermometry

The VTT OxyTherm system was developed during the GeoMetre project as an outdoor-capable thermometer able to measure absolute mean temperature in real time from the path of laser beam, thus solving the problem of unknown effective air refractive index along distance measured. It works by analysing the absorption spectrum caused by spectral lines of molecular oxygen at wavelengths 760-762 nm, comparing the relative strengths of the absorption peaks. During campaign at Metsähovi and the 250 m baseline WUT200 campaigns it was shown with both CNAM's and PTB's reflector that measurement is possible from the same retroreflector simultaneously with OxyTherm and distance meter. The Oxytherm measurement head is connected to the electronics and rest of the optics with single-mode optical fiber. Figure 1 shows PTB and VTT measurement heads next to each other at WUT200. Figure 2 shows the temperature results with PTB's calibrated classical thermometers distributed along the measurement line, and the Oxytherm results. Temperature measurements over 100 m were performed first during the evening and then 200 m results later during the night. During the 100 m measurements when air temperature is decreasing it is expected that the classical thermometers lag the spectroscopic a little. It is evident from the result that the 0.3 K accuracy target can be achieved.

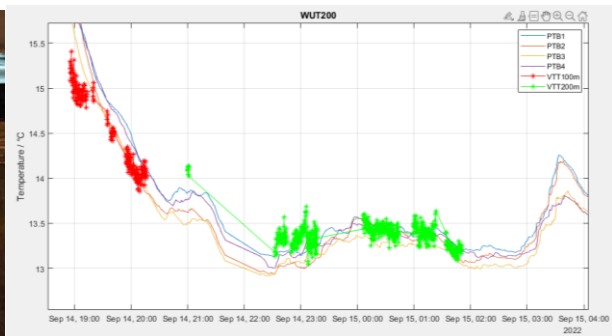


Figure 10 Photos: PTB and VTT (OxyTherm) measurement heads next to each other at WUT200 (Poland), pointed to the same retroreflector target. Data: Comparison of oxytherm observations to readings of the PTB-calibrated classical thermometers

Measurement of vertical gradients

Aside from the varying scale, a maybe lesser-known effect of temperature gradients is the error introduced into optical angular measurements. The refractive index gradient induced by the temperature gradient will cause bending of the optical beams, leading to differences in the true and apparent angles between two points. shows an exaggerated illustration of this effect. This limits the achievable accuracy of the directional measurement essential for optical levelling. To improve the accuracy this effect must be properly compensated.

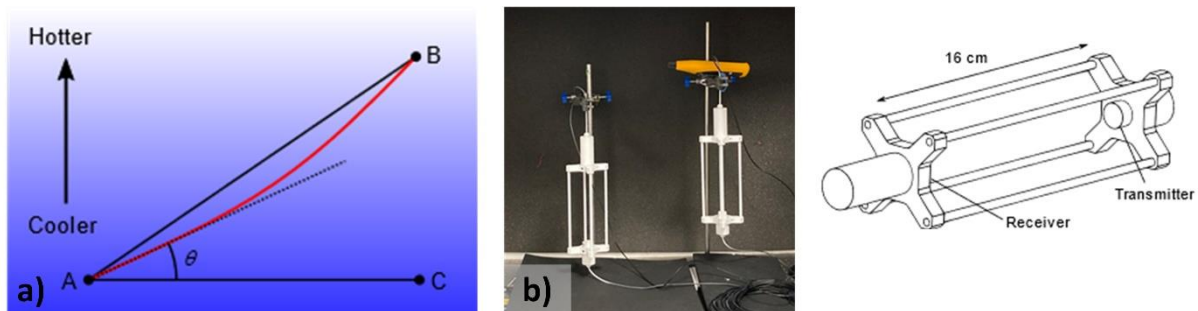


Figure 11 a) Optical beam bending in an air temperature gradient. The apparent angle between points B and C as observed from point A differs from the true angle. b) The acoustic temperature sensor heads in the calibration chamber. Their dimensions are indicated in the diagram on the right-hand side.

Acoustic thermometry is a method, which relies on the dependence of the speed of sound in a gas, u , on thermodynamic temperature, T . Based on previous work, NPL developed a sensor doublet of acoustic temperature sensors to measure vertical temperature gradients in the project. Figure 11b shows a diagram of such a head. It consists of an ultrasonic transmitter and a microphone/preamplifier combination, mounted in a frame and separated by a distance of 16 cm. The frame is built from standard optical cage system components. The frame is designed for dimensional stability, while allowing good airflow in the volume between the transducers. The frame is painted white to reduce the heating effect from solar radiation.

Rather than simply measuring the time-of-flight for an acoustic pulse between the transmitter and microphone, the head is configured to reflect the pulse back and forth between transducer and microphone. The delay which is measured is the time taken for the first reflection from microphone to transducer, and back to microphone – a distance of twice the separation. There are two reasons for using this configuration. Firstly, a bi-direction measurement is needed to mitigate the effects of wind velocity along the axis of the sound beam. Secondly, any errors in measuring the 'trigger time' of the acoustic pulse are eliminated, since only the signal from the microphone is used in determining the time-of-flight.

After validation of the acoustic measurement system in a controlled laboratory environment, NPL shipped the system to the Geodetic Observatory, Wettzell, Germany, for trial air temperature measurements near the radio telescopes for a joint measurement campaign with BKG. The sensors heads were mounted at heights of 4 m and 8 m on a new 10 m mast erected by BKG for the GeoMetre project. A line is suspended from the mast, along which 6 pairs of Pt1000 sensors are mounted at 2 m height intervals. Each pair of Pt1000s has one aspirated and one unventilated (passive) sensor (see Figure 12a). The sensors have a resolution of 0.01 °C and were calibrated in a water bath prior to installation. Figure 12b plots the temperature differences recorded

over the one hour of measurements at daylight. There are several interesting things to note from this plot. Firstly, it is clear how the acoustic sensor system and ventilated Pt1000s both detect fluctuations in difference between the temperature sensors at 8 and 4 m ($T(8m) - T(4m)$) over timescales of minutes, whereas the slow response, and sensitivity to fluctuations in wind speed and solar radiation, of the unventilated Pt1000s masks them. Secondly, the apparent 'noise' in the acoustic readings is larger than the ventilated Pt1000s, but in reality, this reflects the faster response of the acoustic sensor measurement to air temperature fluctuations. The data are a good illustration of how air temperature variations occur on many timescales – from hours, to minutes, to even sub-seconds.

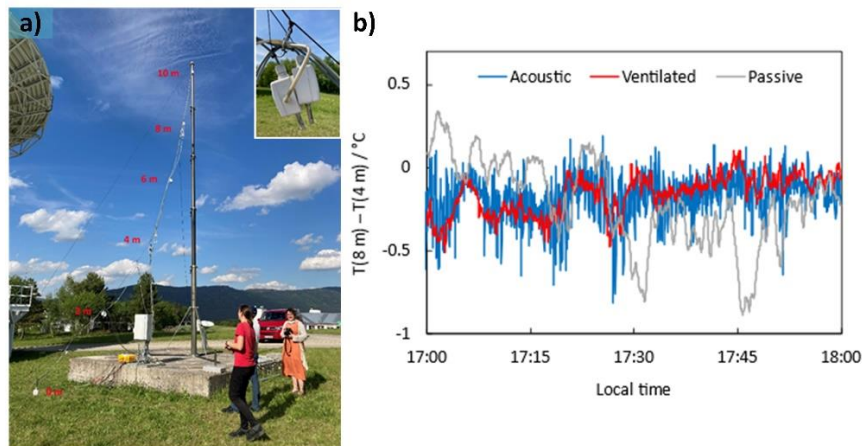


Figure 12 a) The 10 m thermometer mast at Wettzell, with 6 pairs of Pt1000 sensors at 2 m height intervals. Inset: Close-up of a ventilated/passive Pt1000 pair. b) 1-hour plot of temperature differences between 4 m and 8 m heights. Significant differences exist between the passive Pt1000 and the other sensors, indicative of solar loading and a longer response time.

NPL estimates the measurement uncertainty of the temperature difference of the two acoustic sensor to $u(\Delta T_{8m, 4m}) = 0.2 \text{ } ^\circ C$ for the conditions during the measurement. This is comparable to the best uncertainties which could be achieved using contact sensors in this environment while enabling rapid (50 per second) measurements of air temperature differences using acoustics, which in principle is immune to radiative heating effects. For practical surveying work, this comparison results for once clearly underlines the need to work with ventilated sensors when conventional contact sensors are used. But then, the accuracy and response time of these sensors seems sufficient for most applications. Acoustic sensors may have an addition use in detecting rapid, turbulent convection current, which affect the stability of outdoor laser measurement systems.

Summary

The DistriMetre system is a robust multilateration-based system that successfully achieved the targeted uncertainty for the large structures typical for space-geodesy. The consortium explored with the Absolute 3D system an alternative technology route based on interferometry which did not reach the targeted performance during the project lifetime. Besides, the GeoMetre project also pursued alternative approaches such as spectroscopic or acoustic thermometry to deal with more difficult environmental conditions, implying larger gradients in the air index of refraction further. The project could hence deliver an interesting tool set of measurement approaches and instrumentation that can also be combined with classical instrumentation to achieve the targeted measurement uncertainty. The Objective to develop and evaluate at least 1 3D capable novel measurement device with a measurement range of 50 m for outdoor use with the determination of a targeted measurement uncertainty better than $1 \text{ } \mu m / m$ was hence successfully achieved.

Objective 3

To develop technologies, methods and uncertainty assessment for the Earth-bound SI-traceable verification of space-geodetic measurement technologies like GNSS or SLR over distances of at least 5 km with uncertainties of 1 mm or better and their implementation in a European reference standard.

While short-range ($< 1 \text{ km}$) and long-range ($> 10 \text{ km}$) GNSS-based distance measurements are relatively well understood, mid-range distances of several kilometres are a relatively difficult measurement regime if uncertainties of a millimetre and below are targeted. SLR is a time-of-flight based technology, designed for measurement ranges of thousands of kilometres. To perform ground-based verification measurements, references of a few kilometres are necessary not to miss the design working parameters completely. The

optical standards developed for Objective 1 are excellent tools to provide SI-traceable reference distances with low uncertainty for these measurements. In several case studies, the consortium performed such comparison studies, and established a new European reference baseline in Poland.

GBDM+ for GUM-conformal uncertainty assessment of GNSS-based distance measurements

The standard geodetic processing of GNSS measurements (e.g., by Bernese software) does not permit to assess the individual contribution of the different error sources to the final uncertainty in the baseline length. In the GeoMetre project, UPV developed their GNSS-Based Distance-Meter methodology further (GBDM+) They are now able to rigorously estimate the uncertainties in the different error sources affecting each single GNSS measurement used and to analyse their propagation through the equations by which the distance is determined, as well as to deliver the final distance along with its corresponding uncertainty. Their analysis shows that of the leading error sources which persist after double-differencing observations –namely tropospheric and ionospheric delays, multi-path effect and mismodelling of antenna phase centres – multi-path can not only be mitigated but also the uncertainty of its remaining part be estimated by using sidereal filtering and that tropospheric delays can be still substantial after double-differencing. This approach allows a sound metrological treatment of GNSS based distance measurements of several hundreds of metres up to several kilometres.

Verification measurement campaigns at the CERN geodetic reference network



Figure 13 a) CERN geodetic reference network. The five pillars selected for the GeoMetre campaigns are marked by black circles. b) Alignment of a GNSS antenna in preparation of a GBDM+ measurement. c) Arpent system in operation.

Due to the extreme accuracy requirements for the component alignment in high energy physics, CERN maintains one of the best-known geodetic reference networks in the world which has always served as high-level benchmark in the surveying community before. To verify and compare the GBDM+ and Arpent methods, IGN, UPV, CNAM and CERN jointly carried out the measurement campaign. A subset of five pillars from the CERN geodetic network was selected for these campaigns with four baselines of a range between 2.2 and 6.5 km. For the GBDM+ measurement, the four baselines were continuously observed during 3 days. The distance and corresponding uncertainty budget were successfully obtained for each of the baselines. Comparison with data obtained by a Kern Mekometer ME5000 distance meter in the same epoch as well as with other data available from previous campaigns show an overall satisfactory agreement. The distances derived from CNAM's Arpent measurement in separate campaign during the GeoMetre campaign also agree within their expanded measurement uncertainty with the GNSS-based values (see Figure 14).

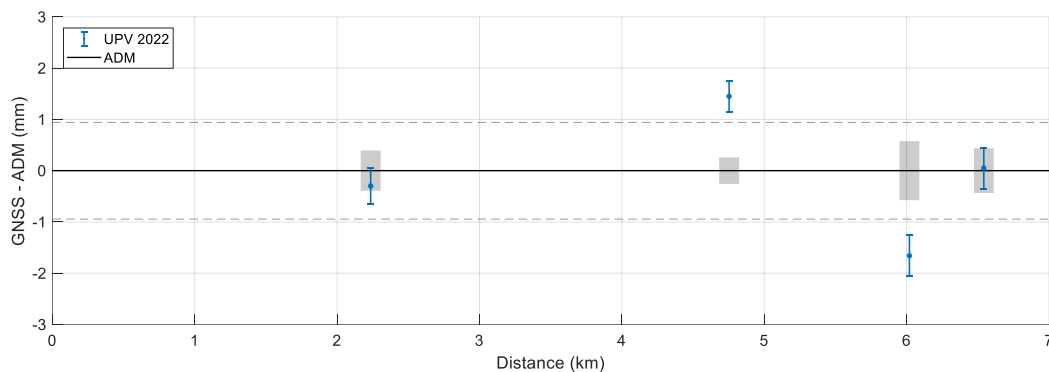


Figure 14 Deviation of CERN baselines measured by GBDM+ (here labelled UPV 2022) from values by the Arpent system (here labeled ADM). The errorbars represent the standard uncertainty (coverage factor $k=1$).

EURO5000 baseline: a new European reference standard for long-distance comparisons

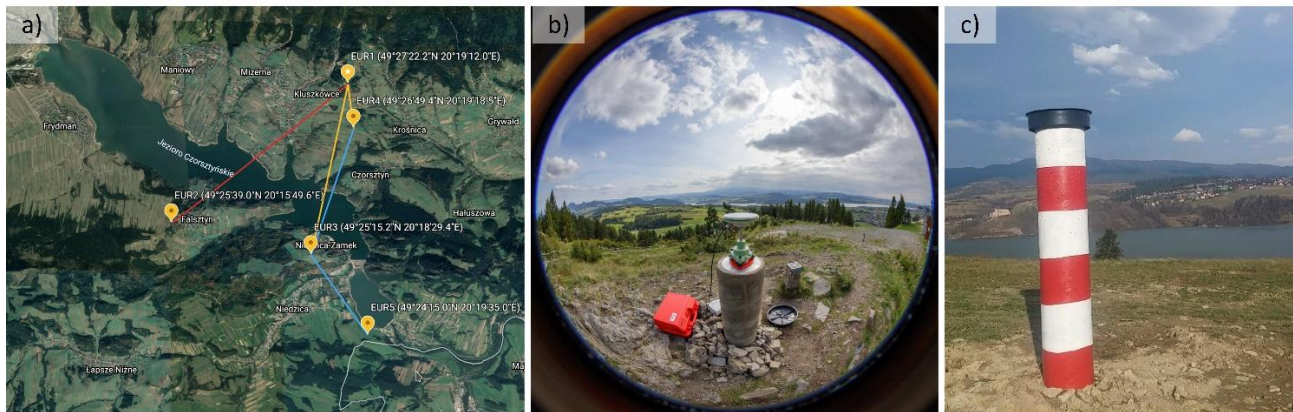


Figure 15 a) EURO baselines in the Pieniny Klippen Belt, Poland established by WUT and GUM during the GeoMetre project. b) GNSS antenna mounted on a reference pillar. c) Newly erected reference pillar.

One key outcome of the GeoMetre project is the establishment of a European reference standard for distance measurements of up to 5 km. WUT and GUM set up this standard, the so-called EURO5000 baseline, within the existing geodynamic test field at the Pieniny Klippen Belt in Poland (Figure 15). During the project, baselines of 1-, 2-, 3-, 4-, and 5-kilometre length were newly built and monitored over three years by GNSS and EDM methods. UPV and CNAM performed measurement campaigns at the EURO5000 using their GBDM+ and Arpent systems. All of these results are compiled in Figure 16. They were used to establish reference coordinates which are given in Table 4. The E_n criterion, the established criterion for the degree of equivalence for such comparison of different methods, is below 1.0 for all data sets, also confirming the measurement uncertainties claimed for the different measurements. For future calibration measurements on the EURO5000 baseline, measurement uncertainty budgets conformal to the Guide to the Expression of Uncertainty in Measurement have been derived for GNSS-based and optical distance meters. The tectonic stability of the area leads to changes of millimetre level between years. Shortly after a fresh calibration of the baseline, however, a measurement uncertainty of better than 1 mm can be achieved for verification measurements up to 5 km.

As mentioned before, the imperfect knowledge of the air refractive index limits the achievable measurement uncertainty for an optical distance measurement. Hence, the achievable uncertainty of a calibration or verification of a commercial electronic distance meter on a geodetic reference baseline strongly depends on the accuracy of the determination of the mean integral refractive index of air \bar{n} . NSC-IM studied the performance of several quadrature methods to approximate the exact integral $\bar{n} = 1/L \int_0^L n(s)ds$ by distributed sensors providing point-wise information on the local environment and gradients. For the linear geodetic polygon, the reference baseline run by NSC-IM at Kharkiv, Ukraine, a relative uncertainty well below 10^{-6} can be achieved corresponding to a level of uncertainty of 1 mm for baseline 5 km. NSC-IM also performed a study how such an improved environmental monitoring system could be implemented to the EURO5000 baseline in future work.

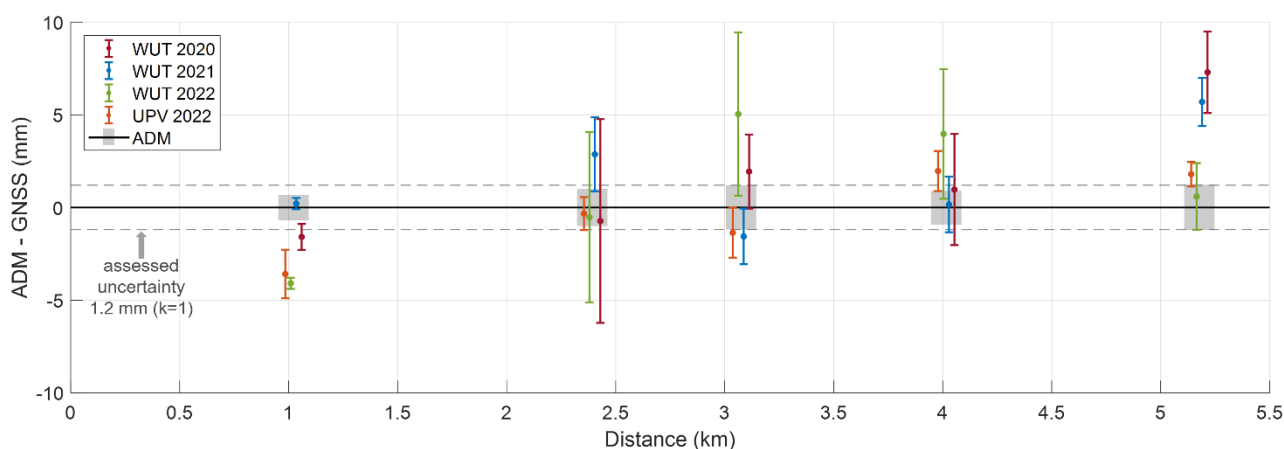


Figure 16 Compilation of the measurement campaigns performed within the GeoMetre project. The results are depicted as deviation from the Arpent observations (labelled ADM in this figure). The error bars indicate standard uncertainties (coverage factor $k=1$).

Table 4 Reference values with their expanded measurement uncertainty ($k=2$) derived from the WUT, UPV and CNAM measurement results.

baseline	d_{WUT}	U_{WUT}	d_{UPV}	U_{UPV}	d_{CNAM}	U_{CNAM}	d_{ref}	U_{ref}
EURO1000	1021,9488	0,0020	1021,9505	0,0013	1021,9469	0,0024	1021,9495	0,0010
EURO2000	2391,9683	0,0039	2391,9706	0,0009	2391,9703	0,0024	2391,9705	0,0008
EURO3000	3074,4443	0,0032	3074,4458	0,0014	3074,4444	0,0024	3074,4453	0,0011
EURO4000	4016,0996	0,0028	4016,0985	0,0011	4016,1005	0,0024	4016,0989	0,0009
EURO5000	5177,1786	0,0043	5177,1774	0,0007	5177,1792	0,0024	5177,1775	0,0006

WUT200: the novel Polish reference baseline for standard surveying equipment

Besides the EURO5000 baseline, a second modern geodetic reference baseline, the WUT200 baseline, was installed and characterized in Poland during the GeoMetre project. The design and infrastructure was made according to ISO standard 16331-1. It consists of seven points which allow verifying the longest distance measurement of 252 m and the additional intermediate distances. WUT and GUM performed calibration measurements using standard surveying equipment like high-end commercial EDMs and laser trackers to determine initial baseline distances. The uncertainty budget derived according to the “Guide to the expression of uncertainty in measurement” (GUM) shows that an uncertainty level below 1 mm is achieved for calibration of standard equipment. In the GeoMetre project, the baseline was used to compare the instrumentation for various refractive compensation methods (acoustic, spectroscopic, and dispersive) at the end of the GeoMetre project. In future, WUT200 will serve as a geodetic reference baseline in Poland to test the uncertainty of standard surveying/geodetic distance measurement equipment.

SLR verification demonstration

Satellite-Laser-Ranging (SLR) is one of the key contributing technologies to the International Terrestrial Reference Frame (ITRF). SLR is the measurement that determines, e.g., the Earth centre for the ITRF. CNRS and OCA are currently revising their SLR instrument and developing it towards two-colour measurement capability. A ground verification of the measurement performance traceable to the SI-definition of the metre with an uncertainty of 1 mm over a range of 2.5 km or more is necessary to support and validate this development. For this purpose, CNRS, OCA, CNAM and IGN developed a comparison in a case study of the GeoMetre project. They compared the performance of the two-colour SLR against a reference measurement by the Arpent system on the OCA premises at Calern, France, using the setup indicated in Figure 17. The Arpent system was mounted close to the SLR telescope (Figure 17a). Both were to measure the distance between two 5'' corner cubes mounted within 5 and 2587 m (Figure 17b). IGN established the local tie between the two measurements (Figure 17c).

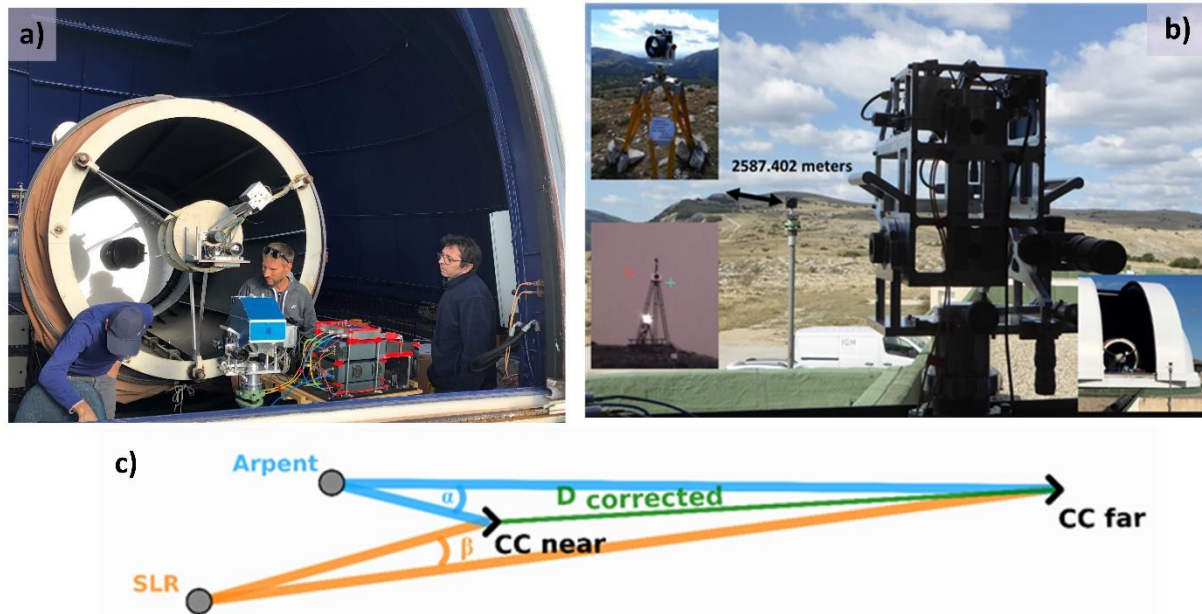


Figure 17 a) Co-location of Arpent and SLR telescope. b) View on the comparison baseline. Small insets: Remote target (cornercube, CC) (left) c) Schematic top view on the comparison design

In the development configuration during the comparison, the OCA SLR achieves a standard measurement uncertainty of 7.6 mm, with an experimental standard deviation for the two-colour system of 3.8 mm. The planned implementation of a new event-timer which will be able to work in continuous mode at a repetition rate of 1 MHz will reduce this uncertainty further. For the comparison scenario sketched in Figure 17, for which uncertainty contribution mutual to both EDM and SLR system like mechanical offsets, e.g., cancel, a measurement uncertainty of 0.83 mm for a coverage factor of $k=2$ could be achieved. A direct comparison was successfully performed for the verification of the scale of the absolute measurement, as well as a resolution test of millimetre steps over a 2.5 km distance (see Figure 18). This joint work will continue, supporting the further development of the OCA SLR system.

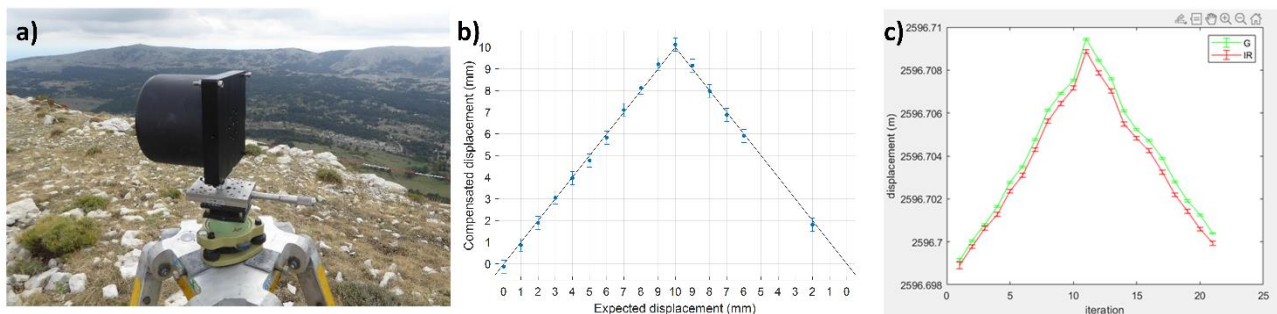


Figure 18 a) Corner-cube mounted in 2.6 km distance on a translational stage which is moved in millimetre steps to investigate displacement accuracy. b) Millimetre steps as observed by the Arpent system in two-colour measurement mode. c) Same movement as observed by the SLR at 532 nm (G) and 1064 nm (IR).

Summary

Despite the challenges of the COVID 19 pandemic situation and the related travelling restrictions, multiple joint long-range comparisons up to 5 km for terrestrial distance and GNSS-based, as well as SLR based distance measurements were developed and performed. Based on the experience gathered in the various campaigns, UPV together with GUM, IGN, NLS, RISE, PTB and WUT wrote a good practice guide on high accuracy GNSS-based distance metrology. They have submitted the document to EURAMET for publication as Technical Guide. The EURO5000 measurement facility will be maintained in future and provides a unique facility to study GNSS-based distance metrology as well as long-range optical systems. Therefore, the Objective to develop technologies, methods and uncertainty assessment for the Earth-bound SI-traceable verification of space-geodetic measurement technologies like GNSS or SLR over distances of at least 5 km with uncertainties of 1 mm or better and their implementation in a European reference standard was successfully achieved.

Objective 4

To reduce uncertainty of the so-called local tie between co-located space-geodetic techniques at GGOS-CS (and all other eligible sites) by one order of magnitude to 1 mm over 200 m in real time continuous tracking. This requires a coordinated effort of novel dimensional measurement systems, methodology and analysis strategies and their demonstration in pilot studies at 2 European GGOS-CS.

The International Terrestrial Reference Frame (ITRF) is based on space-geodetic observations performed worldwide. Each technique, like SLR or VLBI, e.g., operates in its own frame of reference. For the transformation of these observation data into a joint consistent frame of reference – which is the prerequisite for the generation of the ITRF – the local tie vectors are essential. The GeoMetre project has tackled this surveying problem of their measurement from multiple directions: reducing the uncertainty and the SI-traceability of the scale in the surveying networks of co-location sites, developing novel instrumentations and measurement strategies for the reference point determination of the large telescopes, as well as modified analysis strategies. All techniques were investigated at the space-geodetic co-location sites of Metsähovi, Finland, and Wettzell, Germany. Smaller studies were also performed at Onsala, Sweden, and Ny Ålesund, Norway.

The European GGOS core sites Metsähovi and Wettzell

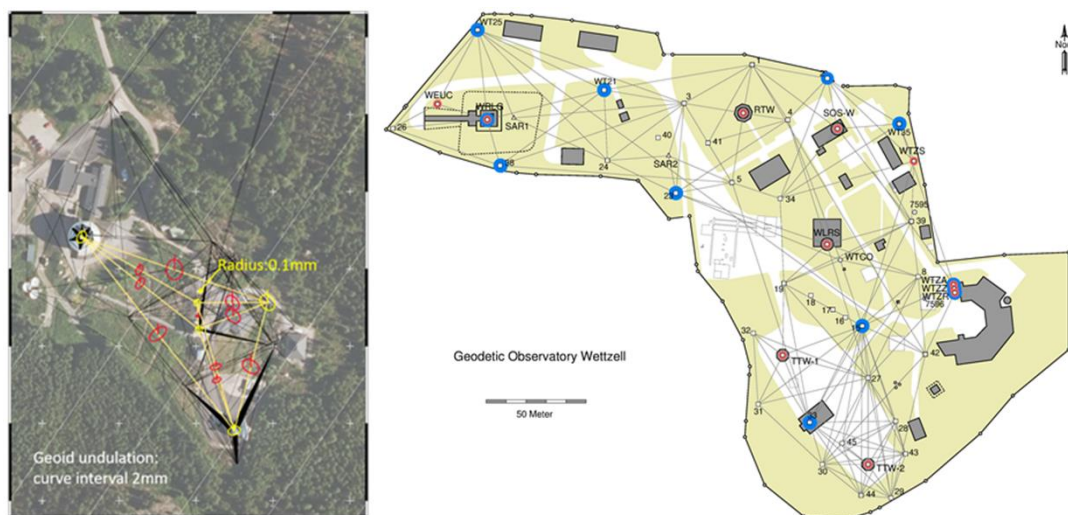


Figure 19 GGOS core site of Metsähovi, Finland (left) and Wettzell, Germany (right). The lines indicate the local terrestrial networks to determine the local tie vectors at these sites.

Two geodetic co-location stations – Metsähovi, Finland, and Wettzell, Germany (Figure 19) - served as case studies for the local tie work in the GeoMetre project. At Metsähovi Geodetic Research Station (MGRS) run by NLS the local tie network consists of four reference points of the space-geodetic instruments: two permanent GNSS antennas (MET3 and MET5) coordinated by the International GNSS Service (IGS), a GGOS VLBI radio telescope and an SLR telescope. Also, the legacy VLBI radio telescope owned by Aalto University is included in the local tie network. During the GeoMetre project, NLS expanded the local survey pillar network by two new masts, which were constructed for the local GNSS and tachymeter network to improve the network geometry. The network distances now vary from 2.5 m to 378 m with a median distance of 49.8 m. The longest distance is to the GNSS point outside the area for better orientation. The scale to the Metsähovi network is traceable to the Nummela standard baseline where the NLS tachymeter and the relevant prisms are calibrated. Special care was taken with so-called micro-local ties at pillars to combine different types of observations. Therefore, NLS established new special adapters at each pillar and mast point enabling the seamless GNSS and tachymeter measurements

The local survey network of the Geodetic Observatory Wettzell (GOW) consists of 30 deeply founded, shielded concrete pillars spread over the entire observatory. Reference points of 3 VLBI radio telescopes, 2 laser ranging telescopes, 5 GNSS antennas and 1 DORIS beacon must be measured and tied together. In the framework of the GeoMetre project, new pillars were established to improve the network geometry: Pillars 43 – 45 to improve the coverage around TTW-2, pillar 42 to realize long distances up to 275 m, and pillar 51 outside the observatory. In addition, a GNSS controlled target at a distance of 5.7 km was erected. Distant targets were included to help reducing the problem of orientation uncertainties on short GNSS baselines. However, the results with the current implementation have provided no significant benefit. As it turns out, due

to the small number of observations to these targets and the loose connection to the local network, the impact on the network orientation is small and the overall standard deviation of the solution increases.

Network scale

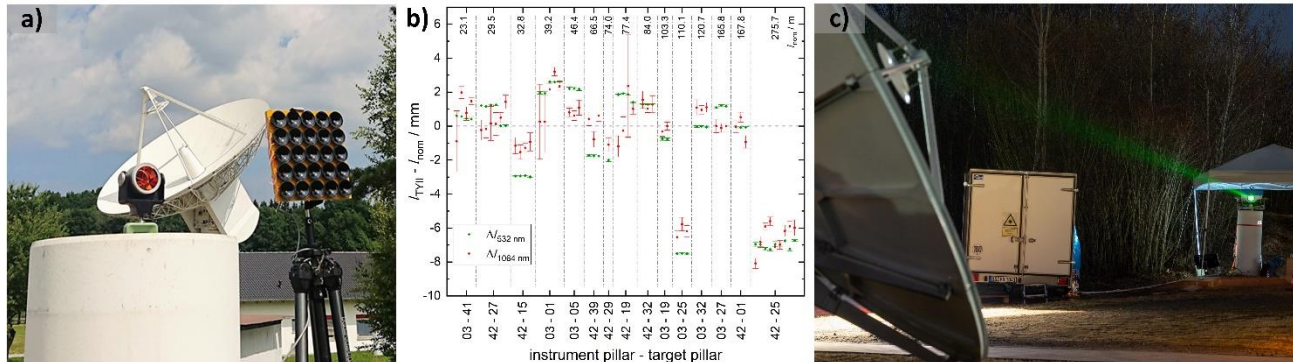


Figure 20 a) The retroreflector fixed on a pillar next to the INRIM array of loudspeakers. b) Preliminary measurement results of the TeleYAG-II measurement campaign at the Wettzell network in March 2022. The error bars indicate the experimental standard deviation of each 10-minute measurement for the highest temporal resolution of 1 ms per measurement. c) The TeleYAG-II instrument mounted on pillar 42 of the Wettzell baseline network.

The local tie vectors connecting the reference points are derived by network adjustments of observations of the permanent surveillance networks installed at the co-location sites (see Figure 19). The uncertainty of the interpillar-distances hence strongly influences the uncertainty of the scale of the local tie vectors, and thus of the whole ITRF adjustment. Therefore, the GeoMetre project deployed its newly developed instrumentations and methods for distance measurements to the reference networks in Metsähovi and Wettzell.

In a first development path, VTT and CNAM combined their spectroscopic thermometer and Arpent measurement system for a joint measurement campaign with NLS at Metsähovi, Finland. Temperatures were measured along two 80 m distances and one 200 m distance. The VTT ‘Oxytherm’ instrument was placed next to the CNAM distance measurement instrument. Temperature and distance were measured along three distances from the pillar on which the CNAM instrument was placed, to three other pillars at the Metsähovi site. The CNAM and VTT instruments used the same retroreflector target that was positioned each time on the target pillar measured. 1-2 classical thermometers were available that could be moved to different places at the site. The measurements at Metsähovi gave temperature readings that seemed to agree with classical point thermometer within ± 0.5 K. A complete analysis of these measurements is still ongoing. A second instrument developed at INRIM allows to measure the average temperature of air between two points by measuring the speed of sound in the path. In June 2022, INRIM and BKG performed a joint measurement campaign at GOW. The experiment consisted in measuring the distance between two pillars with the commercial distance measurement instrument while measuring the air temperature between the same pillars with the acoustic thermometer. Figure 20a shows the loudspeaker array together with the retroreflector mounted on a pillar. The measurement results achieved in the joint campaign show the validity of the concept, but unfavourable conditions limited the output to the measurement of a single baseline only.

Similarly, both Arpent and TeleYAG-II instruments were deployed to joint measurement campaigns with NLS and BKG at Metsähovi, Finland, and Wettzell, Germany, respectively. Both had been successfully verified at geodetic baselines before. Working at the much more difficult environment of co-location sites in mountainous areas proved a severe challenge to the novel systems. Exemplary preliminary results from the TeleYAG-II measurement campaign at Wettzell are compiled in Figure 20b and c. For this campaign, intrinsic two-colour compensation was not possible to be realized due to imperfectly balanced optical glass paths in the interferometer head at the time. To measure the index of refraction, a conventional weather station with five temperature sensors distributed over 200 m was used. Fifteen baselines of the Wettzell network were measured during the campaign, using two pillars (42 and 03) as instrumental basis. Each pair of 532 nm and 1064 nm data depicted in Figure 20b took a measurement time of ten minutes. The error bars in Figure 18a indicates the standard deviation of this raw data without further averaging. The 1064 nm data depicted in red shows a standard deviation which is typically 10 times larger than the data taken at 532 nm. Besides, it is also obvious that the PTB data often deviates in the order of up to 2 mm from the nominal value. The reason for both observations has not yet been clearly identified. Despite the large design effort for temporal robustness of the set-up, temperature changes from -2°C to 20°C ambient temperature proved difficult for the optical set-up. As a result, the quality of the data depicted Figure 20b is not sufficient to improve the accuracy of the

reference network distances. Based on the lessons learned at this campaign, the TeleYAG-II system has been considerably improved since then.

The observation data of the various campaigns were preliminarily included to the network adjustments. Their impact on the adjustment result, however, remains limited for now. For the analysis of the GOW pillar network, in total, more than 7300 terrestrial observations enter. Due to their limited number, the observations by the new instruments have a small weight for the final result. To achieve a larger impact on the network solution, the prototype instruments must be developed to shorter measurement times (and in case of the TeleYAG-II, system, in particular), to faster installation times so that more observations can be performed within reasonable time frames. The collaboration in the field will be continued.

Reference point measurement of permanently installed GNSS antennas

The phase centre of GNSS antennas depend on the individual antenna and the direction of the incoming signal. These corrections to the geometric reference points are generally determined by individual calibrations for which they need to be dismantled and send away. The history of the local tie is hence compromised every time such a calibration takes place. RISE developed a novel method to assess the performance of GNSS absolute antenna calibrations and to determine the phase centres with a combination of inter-antenna differentials and laser tracker measurements. This procedure offers a way to verify the validity of an antenna calibration without touching the antennas and their mounting.

In-process reference point determination

To determine the reference point of a telescope, its elevation and azimuth orientation needs to be varied and telescope angle encoder and observation data simultaneously recorded. The state-of-the-art approach for in-process reference point determination requires a strict synchronisation of both, the measurement system and the telescope. But even then, the uncertainty of the synchronisation can correspond to a position uncertainty of up to 100 $\mu\text{m/m}$ and, therefore, becomes a significant component of the total uncertainty. During the GeoMetre project, Frankfurt UAS developed an approach which does not require synchronisation between the terrestrial instrument and the telescope. It was successfully tested and implemented at GOW, showing negligible deviations from the original approach. As the new approach allows for an in-process metrological determination of the reference point of such space-geodetic techniques and fulfils the GGOS requirements, it provides a major benefit.

SLR reference point monitoring by close-range photogrammetry



Figure 21 Left: SLR antenna moving for the determination of the elevation axis⁹ (reprinted from [16]). Middle: classic determination of the SLR antenna reference point using total stations. Right: determination by close-range photogrammetry.

Frankfurt UAS used close range photogrammetry for the first time to determine the SLR reference point at the GOW in a local frame. For this purpose, a measurement campaign consisting of seven experiments using three different configurations was carried out (see Figure 21). The surrounding of the telescope was equipped with several coded and uncoded markers. To have access to the full uncertainty information of the processing, i.e. the final bundle adjustment, Frankfurt UAS developed the software package JAiCov within the project. The variations of the resulting coordinate components of the reference points are in a range of about ± 0.1 mm with respect to the local datum. Photogrammetry can hence be a good solution for reference point determination as well.

⁹ Reprinted from Lösler et al. (2021) Appl. Sci. 11, 2785

VLBI reference point determination by multilateration

CNAM, BKG, and Frankfurt UAS carried out a joint measurement at GOW in fall 2021 in order to determine the reference point of one of the VLBI radio telescopes. This point has been determined by measuring optical retroreflectors mounted on the rotatable antenna for various azimuth and elevation positions. Basically, the

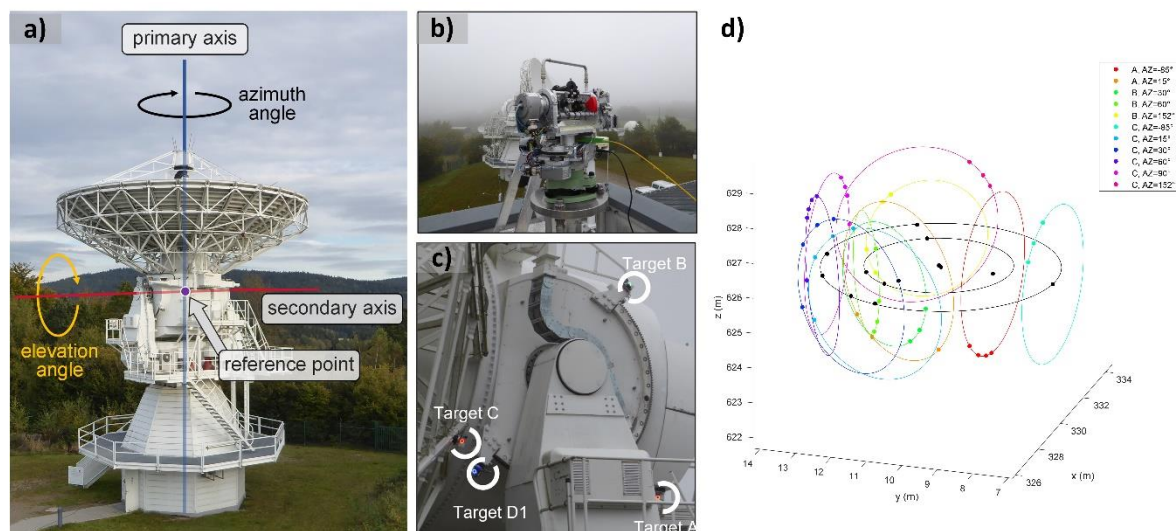


Figure 22 a) The GOW radio telescope TTW-2 of 13.2 m diameter with its two rotating axes. Multilateration set-up with the DistriMetre instrument: b) measurement head, c) target positions. d) Graphical representation of the DistriMetre raw data; full analysis with additional data by Frankfurt UAS

trajectory of these targets allows to model the two rotation axes of the telescope. By this way, the reference point can be determined by an orthogonal projection of the secondary axis onto the primary axis (cf. Figure 22a). DistriMetre, the multilateration system developed and operated by CNAM, has been used for the first time to determine the coordinates of this reference point. Hollow corner cubes were used as targets. Four targets were attached at the structure of the radio telescope by magnetic systems (see Figure 22c). The measuring heads were distributed next to the antenna so that they could all observe a maximum number of targets, simultaneously. During the 9 days of the measurement campaign in Wettzell, 101 target positions were measured with distances ranging from 12 m to 73 m. The multilateration system was exposed to harsh weather conditions during this measurement campaign, with dust and rain that have increased the optical losses and the power fluctuations of the propagated optical beams. In these harsh conditions, the uncertainties on the distance measurements were assessed ($k=1$) between $5.6 \mu\text{m}$ and $43.8 \mu\text{m}$. In 68% of the cases, the uncertainties on the distance measurements are less than $20.6 \mu\text{m}$. For the network adjustment, all the distance measurements of the multilateration system were completed by polar measurements performed by Frankfurt UAS using high-accuracy commercial total stations. This has allowed to increase the number of observations, to cover a larger area of the local site network of GOW, to take into account other space-geodetic techniques and their reference point. All data was analyzed together in a new model developed by Frankfurt UAS. The results show that the accuracy achieved by the DistriMetre multilateration measurement system is at least three times better than the accuracy of a conventional total station. The reference point of the TTW-2 was finally determined by means of least-squares adjustment. The fully populated variance-covariance matrix of the positions obtained from the network adjustment serves as stochastic model within the adjustment. The accuracy achieved for the reference point is considerably better than the targeted GGOS spatial uncertainty of 1 mm.

Deformation monitoring

The large radio telescope structures slightly change their shape when the telescope orientation changes. Gravity-induced deformations of the receiving unit are known to lead to systematic signal path variations (SPV) inducing systematic error on the scale of the VLBI observations. Measuring these deformations is necessary to compensate this effect in the data analysis. Two approaches were followed in the GeoMetre project.

RISE developed a set up combining a 3D scanner mounted on one of the upper supporting leg of a radio telescope (cf. Figure 23b) and an interferometer laser ranger mounted in the telescope centre to track the vertex receiver distance. They deployed their system for the characterization of the 20 m dish at the GGOS co-location site of Ny Ålesund, Norway depicted in Figure 23a. RISE performed five measurement sessions

there, with scans for every 15° elevation angle. The raw data (example in Figure 23c) was fit against a parabolic model, and the elevation dependence given in Figure 23d of the focal length of the radio telescope derived. As an alternative to this approach, Frankfurt UAS and BKG together with Chalmers University, Sweden, and Bochum University of Applied Science investigated the potential of unmanned aerial vehicles (UAV) with studies at GOW and the Onsala Space Observatory, Sweden, for the first time. The components of the receiving unit were measured by means of close-range photogrammetry. Thanks to the UAV, these measurements can be carried out from outside without a crane

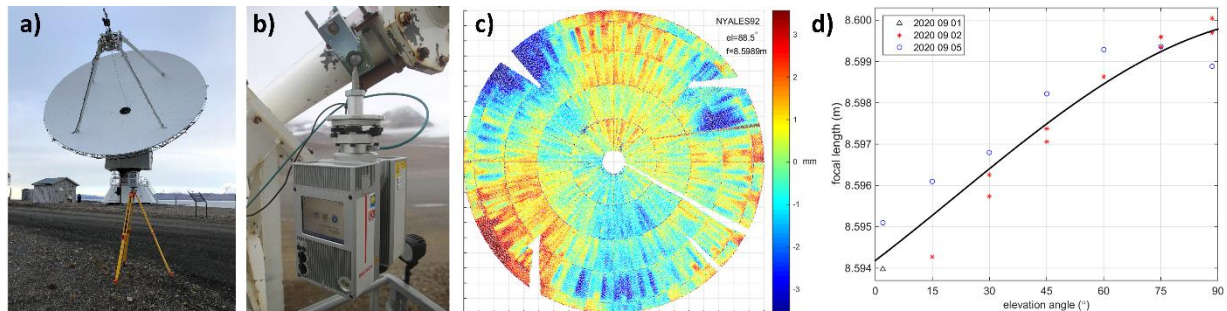


Figure 23 a) 20 m VLBI telescope Ny Ålesund, Norway. b) Laser scanner mounted on upper beam. c) Scan data at 88.5° elevation angle. The colour code indicates the deviation from the average parabola surface. d) Elevation-dependent focal length derived from scans.

and without shading the components of interest of the receiving unit. For the analysis and interpretation of the data, Frankfurt UAS investigated the effect of non-rotationally symmetric deformation patterns for the first time. These deformations occur whenever the optical axis of the whole receiving unit is not identical to the axis of symmetry of each single component of the receiving unit. For the TTW-2 telescope, e.g., they derived an associated maximum delay of less than 3 ps, corresponding to a systematic bias of the vertical coordinate component of about 0.9 mm. Since the Global Geodetic Observing System (GGOS) aims for an accuracy in the position of 1 mm on a global scale, these variations must be accounted for in the analysis.

Network solution

As orientation uncertainties are a major source of error in local tie determination NLS and BKG investigated novel approaches to this problem. In their transformation free approach, BKG works without a local coordinate system. The GNSS coordinates from permanently and temporarily measured pillars are introduced as datum points in the adjustment procedure, and all measured angles which refer to the local plumb line are used after correction of the local deflection of the vertical (DoV). The latter was determined either by an astrogeodetic measurement of the astronomical latitude and longitude, or the gravimetric technique by calculating the surface dip of a fine structure quasi-geoid. Both techniques yield the same DoV with an accuracy of about 1 microrad. In contrast, a purely GNSS based orientation can easily deviate by 30 microrad, assuming a height error of 3 mm over a baseline of 100 m. At Metsähovi, NLS extended the functional model to solve for the instrument orientation at each station point. The angle observations are converted to the local geodetic system at each station point separately using deflections of vertical (DoV) reductions, which were interpolated from the accurate gravimetric quasi-geoid, an updated version of the high-resolution Finnish geoid model, FIN_EIGEN6C4. At both sites the poorly constrained vertical orientation from GNSS observations was significantly improved by the introduction of DoV data in the adjustment of terrestrial observations. This approach can easily be adopted by other geodetic observatories.

In addition, Frankfurt UAS, BKG, and CNAM performed a dedicated comparison study on GOW data obtained in the project on the impact of the analysis approach on the resulting network solution. For that purpose, a procedure is introduced to obtain reference points of space-geodetic techniques defining the local ties. Within the procedure, the reference points are defined independently of the used reference frame and are based on geometrical conditions. Thus, the results depend only on the estimates of the performed network adjustment and the applied network analysis approach. The comparison of the horizontal coordinates of the determined reference points shows a high agreement. The differences are less than 0.2 mm. However, the vertical components differ by more than 1 mm, and exceed the coverage of the estimated standard deviations due to network tilting and network bending.

Summary

The GeoMetre project provided a unique opportunity to investigate novel instrumentation, experimental methods and approaches as well as novel analysis strategies for the local tie metrology problem. Different

perspectives and professional backgrounds led to considerable progress despite delays and problems for the multiple measurement campaigns due to the COVID 19 pandemic situation during the project. Several measures like the improved network solution strategy or the reference point determination led to an immediate reduction of the uncertainty to below the targeted uncertainty of 1 mm for of the local tie vectors and have already been taken up for standard work and contributed to the ITRF2020 solution, others like the TeleYAG-II distance meter need to be developed further before generating considerable impact on the final ITRF product. New bonds formed between the space-geodesy and metrology communities in the project will remain and lead to further collaboration in the future. The consortium achieved the target described in Objective 4 but sees a large potential for future collaboration in this field.

5 Impact

The potential uptake of the project results by end users was promoted by a range of dissemination activities such as presentations at conferences and workshops, and input to metrology committees. The project website presents an overview of the project, together with new updates and announcements, and also provides access to papers, reports and open data produced during the project. The consortium produced and published 38 publications of different types (papers, proceedings, thesis, contributions to books). The major project results were presented in six presentations at two dedicated sessions of the 5th Joint International Symposium on Deformation Monitoring (JISDM) June 8-10, 2022, held in Valencia, Spain.

Impact on industrial and other user communities

This project's primary impact target was a substantial contribution to an improved ITRF solution. First results have already been taken up: a procedure for dynamic reference point determination at SLR and VLBI telescope has been implemented by the Wettzell GGOS core site, and the local gravity field is now considered at Metsähovi and Wettzell for the network adjustment. This capability was also included into a software package used by IGN, a main service provider for these measurements worldwide. Both European core sites also upgraded their surveillance networks. Finally, a new antenna calibration verification procedure that can be performed without removing the antennas can help maintaining continuity in the GNSS network IGS. Beyond, this project developed novel measurement technologies for distance metrology and thermometry in general. These are interesting for the surveying community, as well as automotive, aerospace and wind power industries. Surveying instrument manufacturers, top level surveyors, and European legal metrology benefit from the good practice guide on high-accuracy GNSS-based distance metrology and the novel verification opportunities provided by the new European primary standard network EURO5000. The project has also successfully established close connections with key stakeholders. Two major European GGOS core site operators, the Spanish core site Yebes and the Italian core site Matera, and a representative from GGOS joined the project's stakeholder committee, as well as three major European manufacturers in the field, together with representatives from high energy physics, and measurement science. The consortium organized its kick-off meeting as an open workshop. The results relevant for space geodesy in the field of SLR verification and local tie metrology were presented and discussed at key stakeholder events like the 22nd International Workshop on Laser Ranging, the Reference Frames for Applications in Geosciences (REFAG 2022), or the GGOS Unified Analysis Workshop in autumn 2022.

Impact on the metrology and scientific communities

This project substantially strengthened traceability of the ubiquitous global mapping systems to the SI definition of the metre by reducing the uncertainty of local tie vectors and enabling the SI-traceable verification of SLR measurements at an uncertainty level below 1 mm. Moreover, the project has developed guide on metrologically-sound GNSS-based distance measurements and their realisation with low uncertainty. Furthermore, European NMIs will be able to offer novel services. Laser scanning assisted VLBI antenna deformation monitoring has already being provided by RISE as a direct outcome of their project work. Improved surveying instrument calibration and verification are possible at Europe's first metrology-grade baseline over 5 km, as well as at the novel 250 m baseline for shorter distances. Furthermore, the primary standards developed in the project for long range 1D measurements and 3D capable measurement devices enable the calibration of respective national standards, like large-scale coordinate measurement machines or geodetic baselines. Project results have already been presented at thirty-nine contributions to international conferences, leading to fifteen peer-reviewed conference proceedings papers. Twenty-two manuscripts have been accepted and published by high-ranking peer-reviewed international journals.

Impact on relevant standards

The project was represented in twelve standardisation bodies in the field of space geodesy and surveying. These included ISO and national standardisation bodies, but also IAG and IERS working groups or national surveying organizations. IAG e.g., has been informed about the project's discovery of the error in the original Ciddor and Hill algorithm for group refractive index compensation. Members of the IERS Working Group on Site Survey and Co-location were addressed by contributions to the REFAG 2022 and the GGOS Unified Analysis Workshop 2022. The ISO working groups ISO TC211 "Geographic information/Geomatics, the IERS Working Group on Site Survey and Co-location, and the ISO TC172 SC06 "Optics and photonics – geodetic and surveying instruments" were addressed by representation at their meetings as well as presentations at respective national mirror bodies. As a major impact on standardization, EURAMET TC-L has launched Euramet project 1572 with the target to adopt the GNSS best practice guide as EURAMET Technical Guide.

Longer-term economic, social and environmental impact

The UN GA has acknowledged the great importance of geodetic reference frames. Considerable advance was generated in the field of local tie metrology. Many of the outcomes can easily applied by the 15 GGOS-CS and other eligible co-location sites world-wide. This can help to improve future ITRF solutions. Improved quality of the reference networks (as well as of optical measurement equipment) will enhance the capability to monitor critical sites, e.g., future nuclear waste repositories or carbon sequestration repositories, and construction engineering projects such as bridges, dams, tunnels, and roads in mountainous regions. Most importantly, lower uncertainties in geodetic surveillance data will empower Earth science to draw reliable conclusions faster, e.g., on the real velocity of glacier retreat in Greenland, or on the rise of global sea levels. The project hence made a small, but significant contribution to a better understanding of these globally important environmental changes.

6 List of publications

1. M. Lösler, C. Eschelbach, S. Riepl and T. Schüler, "Zur Bestimmung des ILRS-Referenzpunktes am Satellite Observing System Wettzell", in „Photogrammetrie - Laserscanning - Optische 3D-Messtechnik: Beiträge der 18. Oldenburger 3D-Tage 2019“, Edition: 1, Chapter: Messtechnik und Scansysteme, Publisher: Wichmann Verlag, pp.162-175 (2019) <https://doi.org/10.5281/zenodo.3515831>
2. M. Lösler, R. Haas, C. Eschelbach and A. Greiwe, "Gravitational deformation of ring-focus antennas for VGOS: first investigations at the Onsala twin telescopes project", Journal of Geodesy 93, 2069-2087 (2019) <https://doi.org/10.1007/s00190-019-01302-5>
3. M. Lösler, C. Eschelbach, R. Haas and A. Greiwe, "Measuring Focal Length Variations of VGOS Telescopes Using Unmanned Aerial Systems" in Proceedings of the 24th European VLBI Group for Geodesy and Astrometry Working Meeting, 17-19 March 2019, Las Palmas de Gran Canaria, Spain, Eds. R. Haas, S. Garcia-Espada, and J. A. López Fernández, pp. 17-21 (2019) <https://doi.org/10.7419/162.08.2019>
4. M. Lösler, C. Eschelbach, S. Riepl and T. Schüler, "A Modified Approach for Process-Integrated Reference Point Determination" in Proceedings of the 24th European VLBI Group for Geodesy and Astrometry Working Meeting, 17-19 March 2019, Las Palmas de Gran Canaria, Spain, Eds. R. Haas, S. Garcia-Espada, and J. A. López Fernández, pp. 172-176 (2019) <https://doi.org/10.7419/162.08.2019>
5. J. Guillory, D. Truong and J.-P. Wallerand, "Assessment of the mechanical errors of a prototype of an optical multilateration system", Review of Scientific Instruments 91, 025004 (2020) <https://doi.org/10.1063/1.5132933>
6. Y. Liu, A. Röse, G. Prellinger, P. Köchert, J. Zhu and F. Pollinger, "Combining Harmonic Laser Beams by Fiber Components for Refractivity-Compensating Two-Color Interferometry," Journal of Lightwave Technology, Vol 37, No 7 (2020) <https://doi.org/10.1109/JLT.2019.2960473>
7. A. Röse, Y. Liu, P. Köchert, G. Prellinger, E. Manske, and F. Pollinger, "Modulation-based long-range interferometry as basis for an optical two-color temperature sensor," in Proceedings of euspen's 20th International Conference & Exhibition, June 2020 <https://doi.org/10.7795/EMPIR.18SIB01.CA.20200818>
8. C. Eschelbach, M. Lösler, R. Haas, and A. Greiwe, "Untersuchung von Hauptreflektordeformationen an VGOS-Teleskopen mittels AUS," in Ingenieurvermessung 20: Beiträge zum 19. Internationalen

- Ingenieurvermessungskurs, March 2020 <https://doi.org/10.5281/zenodo.4081146>
9. P. Neyezhnikov, V. Kupko, T. Panasenkov, A. Prokopov, V. Skliarov, and A. Shloma, "Analysis of accuracy requirements to the meteorological sensors used to compensate for the influence of the Earth's atmosphere in high precision length measurement," in Proceedings of SMSI Sensor and Measurement Science International (2020) <https://doi.org/10.5162/SMSI2020/D3.3>
 10. S. Bergstrand, P. Jarlemark, M. Herbertsson, "Quantifying errors in GNSS antenna calibrations – towards in situ phase center corrections," *J Geod* 94, 105 (2020) <https://doi.org/10.1007/s00190-020-01433-0>
 11. F. Pollinger, "Refractive index of air. 2. Group index: comment," *Appl. Opt.* 59, 9771-9772 (2020) <https://doi.org/10.1364/AO.400796>
 12. M. Lösler, „Zur Parameterschätzung mit unterschiedlichen Koordinatendarstellungen, Zeitschrift für Geodäsie,“ *Geoinformatik und Landmanagement (ZfV)*, Vol. 145(6), S. 385-392 (2020) <https://doi.org/10.12902/zfv-0319-2020>
 13. P. Neyezhnikov, T. Panasenkov, A. Prokopov, V. Skliarov, A. Shloma, I. Trevoho, "Comparative analysis of quadrature formulas for the mean integral refractive index of air in high-precision ranging", *Modern achievements of geodesic science and industry* 39, pp. 69-73 (2020) <https://doi.org/10.33841/1819-1339-1-39-13>
 14. M. Lösler, „Modellbildungen zur Signalweg- und in-situ Referenzpunktbestimmung von VLBI-Radioteleskopen,“ PhD Thesis published at TU Berlin (2020) <https://doi.org/10.14279/depositonce-11364>
 15. J. Guillory, D. Truong, J.-P. Wallerand, „Uncertainty assessment of a prototype of multilateration coordinate measurement system,“ *Precision Engineering*, Vol 66, 496-506 (2020) <https://hal-cnam.archives-ouvertes.fr/hal-03190544>
 16. M. Lösler, C. Eschelbach, T. Klügel, S. Riepl, "ILRS Reference Point -Determination using Close Range Photogrammetry," *Appl. Sci.* 2021, 11(6), 2785 (2021) <https://doi.org/10.3390/app11062785>
 17. A. Röse, P. Köchert, G. Prellinger, F. Pollinger, „Monte-Carlo Analysis of Challenges and Limitations of Dispersion-based Optical Thermometry,“ in Proceedings of SMSI Sensor and Measurement Science International (2021) <https://doi.org/10.5162/SMSI2021/C4.4>
 18. F. Pilarski, F. Schmaljohann, S. Weinrich, J. Huisman, D. Truong, T. Meyer, P. Köchert, R. Schödel, F. Pollinger, "Design and manufacture of a reference interferometer for long-range distance metrology," in Proceedings of euspen's 21st International Conference & Exhibition, June 2021 <https://www.euspen.eu/knowledge-base/ICE21222.pdf>
 19. J. Guillory, D. Truong, J.-P. Wallerand, C. Alexandre, "Absolute multilateration-based coordinate measurement system using retroreflecting glass spheres," *Precision Engineering*, Volume 73, Pages 214 – 227 (2021) <https://doi.org/10.1016/j.precisioneng.2021.09.009>
 20. P. Neyezhnikov, A. Prokopov, T. Panasenkov, V. Skliarov, A. Shloma, "Towards the assessment of the accuracy of measuring the integral characteristics of physical quantities using the sensors of discrete values of these quantities" in Proceedings of SMSI Sensor and Measurement Science International (2021) <https://doi.org/10.5162/SMSI2021/C9.2>
 21. L. García-Asenjo, S. Baselga, C. Atkins, P. Garrigues "Development of a Submillimetric GNSS-Based Distance Meter for Length Metrology," *Sensors* 2021, 21(4), 1145 (2021) <https://doi.org/10.3390/s21041145>
 22. M. Lösler, C. Eschelbach, C. Holst, "On the Impact of the Coordinate Representation onto the Estimates in Least-Squares Adjustment," in Proceedings of the 25th European VLBI for Geodesy and Astrometry (EVGA) Working Meeting, 14.-18. March 2021, Chalmers University of Technology, Gothenburg, Sweden, pp. 49-55 (2021) <https://doi.org/10.5281/zenodo.5811948>
 23. F. Pollinger, et al., "Large-Scale Dimensional Metrology for Geodesy—First Results from the European GeoMetre Project," in: *International Association of Geodesy Symposia*. Springer, Berlin, Heidelberg (2022) https://doi.org/10.1007/1345_2022_168
 24. U. Kallio, T. Klügel, S. Marila, S. Mähler, M. Poutanen, T. Saari, T. Schüller, H. Suurmäki, "Datum Problem Handling in Local Tie Surveys at Wettzell and Metsähovi," in: *International Association of Geodesy Symposia*. Springer, Berlin, Heidelberg (2022) https://doi.org/10.1007/1345_2022_155
 25. S. Baselga, L. García-Asenjo, P. Garrigues, R. Luján, "GBDM+: an improved methodology for a GNSS-based distance meter," *Meas. Sci. Technol.* 33 085020 (2022)

- <https://iopscience.iop.org/article/10.1088/1361-6501/ac6f45>
26. J. Guillory, D. Troung, J.-P. Wallerand, "Multilateration with Self-Calibration: Uncertainty Assessment, Experimental Measurements and Monte-Carlo Simulations," *Metrology* 2, no. 2: 241-262 (2022) <https://doi.org/10.3390/metrology2020015>
 27. K. Wezka, L. García-Asenjo, D. Próchniewicz, S. Baselga, R. Szpunar, P. Garrigues, J. Walo, R. Luján, "EDM-GNSS distance comparison at the EURO5000 calibration baseline: preliminary results", *Journal of Applied Geodesy* (2022) <https://doi.org/10.1515/jag-2022-0049>
 28. L. García-Asenjo, S. Baselga, P. Garrigues, R. Luján, D. Pesce, B. Weyer, J.F. Fuchs, D. Missiaen, "Application of GNSS length metrology to CERN geodetic network," in *Proceedings IWAA 2022, International Workshop on Accelerator Alignment* (2022) <https://indico.cern.ch/event/1136611/contributions/5020510>
 29. M. Lösler, C. Eschelbach, S. Mähler, J. Guillory, D. Truong, J.-P. Wallerand, "Operator-software impact in local tie networks", *Appl Geomat* (2023) <https://doi.org/10.1007/s12518-022-00477-5>
 30. M. Lösler, C. Eschelbach, A. Greiwe, R. Brechtken, C. Plötz, G. Kronschnabl, A. Neidhardt, "Ray tracing-based delay model for compensating gravitational deformations of VLBI radio telescopes" *Journal of Geodetic Science*, vol. 12, no. 1, pp. 165-184 (2022) <https://doi.org/10.1515/jogs-2022-0141>
 31. P. Nyezshmakov, O. Prokopov, T. Panasenko, A. Shloma, "Analysis of the temperature component of the combined standard uncertainty of the refractive index according to the test data of the control system for meteorological parameters developed for the Lyptsi geodetic polygon", *Ukrainian Metrological Journal* 4, pp. 34-38 (2021) <https://doi.org/10.24027/2306-7039.4.2021.250411>
 32. P. Nyezshmakov, O. Prokopov, T. Panasenko, A. Shloma, "Comparative analysis of the accuracy requirements of the equipment for determining the mean integral refractive index of air using different realizations of the gradient method", *Ukrainian Metrological Journal* 2, pp. 20-24 (2021) <https://doi.org/10.24027/2306-7039.4.2021.250411>
 33. U. Kallio, J. Eskelinen, J. Jokela, H. Koivula, S. Marila, J. Näränen, M. Poutanen, A. Raja-Halli, P. Rouhiainen, H. Suurmäki, "Validation of GNSS-based reference point monitoring of the VGOS VLBI telescope at Metsähovi", in *Proceedings of the 5th Joint International Symposium on Deformation Monitoring – JISDM 2022, June 20-22, 2022, Valencia, Spain*, pp. 93-98 (2023) <https://doi.org/10.4995/JISDM2022.2022.13691>
 34. C. Eschelbach, M. Lösler, "A feasibility study for accelerated reference point determination using close range photogrammetry", in *Proceedings of the 5th Joint International Symposium on Deformation Monitoring – JISDM 2022, June 20-22, 2022, Valencia, Spain*, pp. 1-8 (2023) <https://doi.org/10.4995/jisdm2022.2022.13417>
 35. J. Guillory, D. Truong, J.-P. Wallerand, "Optical distance measurements at two wavelengths with air refractive index compensation", in *Proceedings of the 5th Joint International Symposium on Deformation Monitoring – JISDM 2022, June 20-22, 2022, Valencia, Spain*, pp. 151-157 (2023) <https://doi.org/10.4995/JISDM2022.2022.13786>
 36. A. Sauthoff, P. Köchert, G. Prellinger, T. Meyer, F. Pilarski, S. Weinrich, F. Schmaljohann, J. Guillory, D. Truong, J. Silbermann, U. Kallio, J. Jokela, F. Pollinger, "Two multi-wavelength interferometers for large-scale surveying", in *Proceedings of the 5th Joint International Symposium on Deformation Monitoring – JISDM 2022, June 20-22, 2022, Valencia, Spain*, pp. 31-39 (2023) <https://doi.org/10.4995/JISDM2022.2022.13635>
 37. M. Pisani, M. Astrua, A. Merlone, "Non-Contact Thermometer for Improved Air Temperature Measurements", *Sensors* 2023, 23, 1908 (2023) <https://doi.org/10.3390/s23041908>
 38. F. Pollinger, S. Baselga, C. Courde, C. Eschelbach, L. García-Asenjo, P. Garrigues, J. Guillory, P. O. Hedekvist, T. Helojärvi, J. Jokela, U. Kallio, T. Klügel, P. Köchert, M. Lösler, R. Luján, T. Meyer, P. Nyezshmakov, D. Pesce, M. Pisani, M. Poutanen, G. Prellinger, A. Sauthoff, J. Seppä, D. Truong, T. Underwood, K. Wezka, J.-P. Wallerand, M. Wiśniewski, "The European GeoMetre project: developing enhanced large-scale dimensional metrology for geodesy", *Appl Geomat* (2023) <https://doi.org/10.1007/s12518-022-00487-3>

7 Contact details

Florian Pollinger, PTB, florian.pollinger@ptb.de